

AD-A054 754

CHARLES STARK DRAPER LAB INC CAMBRIDGE MA F/G 22/3
OPTIMAL ESCAPE TRAJECTORY FROM A HIGH EARTH ORBIT BY USE OF SOL--ETC(U)
AUG 77 A J GREEN

F/G 22/3

UNCLASSIFIED

T-652

NL

1 OF 2
AD
A054754

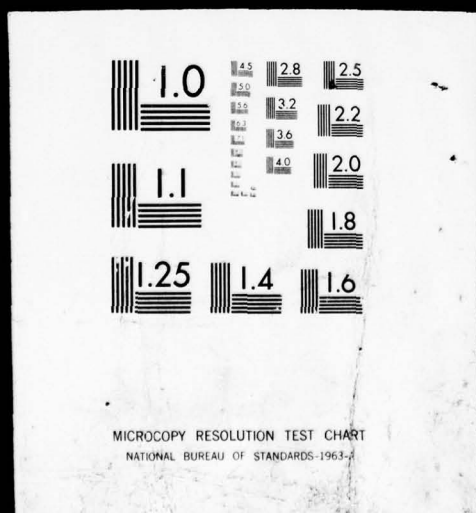


100

1 OF 2

AD

A054754



AD No. AD A 054754
DDC FILE COPY

FOR FURTHER TRAN *EW*

①
5C

⑥

⑭ T-652

OPTIMAL ESCAPE TRAJECTORY FROM A HIGH EARTH
ORBIT BY USE OF SOLAR RADIATION PRESSURE

by

⑩ Andrew Joseph Green

⑪ 8 August 1977

Master of Science Thesis
Massachusetts Institute of Technology

⑫ 106p.

⑨ Master's thesis,



The Charles Stark Draper Laboratory, Inc.

Cambridge, Massachusetts 02139

DISTRIBUTION STATEMENT A
Approved for public release;
Distribution Unlimited

DDC
REF ID: A
JUN 9 1978
408 386 1B

OPTIMAL ESCAPE TRAJECTORY FROM A HIGH EARTH ORBIT
BY USE OF SOLAR RADIATION PRESSURE

by

Andrew Joseph Green

A.S., Mohawk Valley Community College
(1970)

B.S., United States Military Academy
(1974)

SUBMITTED IN PARTIAL FULFILLMENT

OF THE REQUIREMENTS FOR THE

DEGREE OF

MASTER OF SCIENCE

at the

MASSACHUSETTS INSTITUTE OF TECHNOLOGY

September 1977

Signature of Author

Andrew J. Green
Department of Aeronautics and Astronautics,
24 August 1977

Certified by

Louis A. D'Amato

Thesis Supervisor

Certified by

Donald C. Chase

Thesis Supervisor

Accepted by

*Chairman, Departmental Committee on
Graduate Studies*

OPTIMAL ESCAPE TRAJECTORY FROM A HIGH EARTH ORBIT

BY USE OF SOLAR RADIATION PRESSURE

by

Andrew Joseph Green

ACCESSION NO.	
RTIS	White Section <input checked="" type="checkbox"/>
DBS	Buff Section <input type="checkbox"/>
UNANNOUNCED	
JUSTIFICATION	
Litter on file	
DISTRIBUTION AVAILABILITY CODES	
DIR.	AVAIL. REG. OR SPECIAL
<i>A</i>	

Submitted to the Department of Aeronautics and Astronautics
on 24 August 1977, in partial fulfillment of the requirements
for the degree of Master of Science.

ABSTRACT

↓ This thesis develops the optimal control law necessary for a minimum time escape from a high Earth orbit utilizing solar radiation pressure. A force model is developed for an ideal flat sail and a proposed Jet Propulsion Laboratory square sail. A two-body inverse square force field model is assumed. The Earth's orbit about the Sun is assumed circular, and the solar flux is assumed constant during the escape maneuver. The initial state is given, and the only condition on the final state is that the energy of the spacecraft equals zero. A modified Newton-Raphson method is used to solve the two-point boundary value problem. It is found that the performance of any solar sail escape trajectory tends to fall between the limiting cases of similar polar and ecliptic escape trajectories. A velocity-dependent control law is also examined and found to be a good approximation to the optimal control law. ↗

Thesis Supervisor: Donald C. Cleary
Title: Lecturer

DEDICATED TO:

Theodore N. Edelbaum

ACKNOWLEDGMENTS

I wish to thank the United States Army and the Fannie and John Hertz Foundation for making it possible for me to continue my education. I would also like to express my gratitude to Lester L. Sackett and Louis A. D'Amario for their help, encouragement and understanding during this research.

CONTENTS

	<u>Page</u>
List of Symbols-----	1
Chapters	
1. Introduction	
1.1 Background-----	4
1.2 Objective-----	4
1.3 Synopsis-----	6
2. Force Model	
2.1 General Force Model-----	7
2.2 JPL Force Model-----	12
2.3 Effects of Solar Wind and Earth Shine-----	15
3. Optimization	
3.1 Coordinate System-----	18
3.2 Constraints-----	19
3.3 The Optimal Control Law-----	20
3.4 Boundary Conditions-----	27
3.5 Summary-----	29
4. Discussion	
4.1 Introduction-----	31
4.2 Optimal Control-----	33
4.3 Open-Loop Control-----	36
4.4 Velocity-Dependent Control-----	37
5. Conclusions-----	49
Bibliography-----	51
Appendices	
A. Force Equation Parameters-----	54
B. Optimal Control Theory-----	61
C. An Energy Dependent Newton-Raphson Iterator-----	66
D. Computer Program-----	71

LIST OF SYMBOLS

a - absorption coefficient
 a_c - characteristic acceleration
 a_c - acceleration on the sail due to solar radiation pressure
A - area of sail
 B_f, B_g - non-Lambertian coefficients of front and back surfaces
c - speed of light
 c_1, c_2, c_3 - sail force coefficients
 C_R, C_i^R - rotation matrix
E - energy
 E_a - sunlight power absorbed by Earth
 E_{RE} - re-radiated Earth power
F - total radiation force
 F_a - force due to absorption
 F_r - force due to reflection
 F_r - force due to re-radiation
 F_o - maximum force at 1 A.U. from the Sun
g - gravity
H - Hamiltonian
 $HP = \frac{\partial H}{\partial p}$
 $HPP = \frac{\partial^2 H}{\partial p^2}$
h - Plank's constant
 \mathbf{i} - unit vector in the direction of the x-axis
 \mathbf{j} - unit vector in the direction of the y-axis
J - performance index
 \mathbf{k} - unit vector in the direction of the z-axis

L - integrand of the performance index
 \underline{m} - unit vector in the direction of spectrally reflected sunlight
 \underline{n} - unit vector normal to sail's surface
 m - mass of sail
 p - solar pressure
 P_s - solar intensity
 P_{sw} - solar wind intensity
 P_{ee} - intensity of re-radiated energy from Earth
 P_{es} - Earth shine intensity
 r - reflectivity of sail's surface or magnitude of radius vector
 r_e - albedo of Earth
 \underline{r} - radius vector
 R - distance of spacecraft from the Sun
 R_g - distance of Earth from the Sun
 R_e - radius of the Earth
 s - specular reflection coefficient
 S - terminal cost function of the performance index
 t - time
 T - temperature
 \underline{v} - velocity vector
 V_c - circular orbital velocity
 \underline{x} - state of the spacecraft

α - angle between the normal of the sail and $-\underline{i}$
 β - cone angle of \underline{d}_v
 β_L - limiting cone angle
 γ - angle of Sun with respect to the inertial coordinate frame

ξ, ϵ_B - emissivity of the front and back surface
 \hat{f} - unit vector in the direction of the radiation force
 $n(\nu)$ - photons per unit area per unit time per unit frequency
 $\hat{\gamma}$ - unit vector tangent to the sail's surface
 Θ - cone angle of the radiation force vector
 Θ_c - limiting cone angle
 λ - co-state vector
 λ_r - position co-state vector
 λ_v - velocity co-state vector
 μ - gravitational constant
 ν - frequency of photon or angle or Lagrange multiplier
 σ - Stefan-Boltzman constant or clockangle of λ_v
 τ - transmissivity of surface
 ϕ - centerline angle
 ψ - clockangle of the radiation force vector
 ω - rotation rate of Earth about the Sun

Superscripts

i - with respect to the inertial coordinate frame
 n - n^{th} term or variable
 T - transpose of the matrix
 R - with respect to the rotating coordinate frame

Subscripts

o - initial
 f - final
 r - of or pertaining to the radius vector
 v - of or pertaining to the velocity vector

1. INTRODUCTION

1.1 Background

A solar sail is a device which creates a propulsive force from solar radiation pressure. The solar radiation pressure results from changes in the momentum of incident photons on the sail's reflective surface. This force can be used to increase or decrease the energy of the solar sail, thereby allowing travel in the vicinity of the radiation source.

One of the first examinations of a solar sail powered vehicle supposedly occurred in a paper by the Russian author, F.A. Tsander, in 1924(ref 3). It was not until the late 1950's that serious interest in the concept of solar sail propulsion occurred. The majority of the papers written on solar sail propulsion have been concerned with the solar sail as a means of interplanetary travel. The use of a solar sail as a means of planetary escape has been considered(ref 4 and 11), but the analysis has been rather restricted.

Since the Space Shuttle program is envisioned to make low Earth orbits readily attainable, the solar sail is at present being considered for various high Earth orbit and interplanetary missions. The solar sail is rather interesting in regards to interplanetary travel in that it has the potential for improved performance over interplanetary ballistic and solar electric propulsion systems. Inherent to any interplanetary mission is the successful escape from Earth.

1.2 Objective

Since the solar sail draws its energy from a limitless

source, the optimal escape trajectory from Earth should be the trajectory that reaches escape in the minimum time. A straight numerical integration of the equations of motion, in order to determine the optimal trajectory, usually results in numerical problems. These numerical problems are due to a large escape time (in the order of months) and to the small integration time step needed. The method of averaging the orbital elements as discussed in references 8, 9, and 10, has proved successful in the determination of optimal orbit raising trajectories. As the ratio of the propulsive force to the local gravitational force becomes large, the method of averaging becomes inaccurate. For the solar sails discussed in Appendix A, it appears that the method of averaging should be terminated when the trajectory reaches the vicinity of 100000 kilometers from the center of the Earth. It is therefore the purpose of this thesis to develop an analytical model that will calculate the control law necessary for a minimum time escape from a high Earth orbit with a solar sail. It is felt that a model similar to the one presented in this thesis could be combined with an averaging method to determine the complete optimal escape trajectory of a solar sail from a low Earth orbit.

Some basic assumptions are made in the solution of this problem:

1. The state is completely given at the time of launch.
2. The solar flux is constant during the escape maneuver.
3. The distance between the Sun and the spacecraft is equal to the distance between the Sun and Earth.

4. The Earth's orbit about the Sun is circular.
5. The Earth has an inverse square gravitational field.
6. The only gravitational field which affects the space-craft is that of the Earth.
7. The effects of Earth shadowing is neglected.

1.3 Synopsis

This thesis is divided into five chapters. Chapter one is the introduction. Chapter two develops an equation for the magnitude and direction of the resultant force on a solar sail due to solar radiation pressure. Chapter three develops the differential equations of motion for the state and co-state. Optimal control theory is applied to determine expressions for the time history of the control variables and the necessary boundary conditions on the co-state. Chapter four explains some of the results of optimal control escape trajectories. Two other types of control laws, open-loop control and velocity-dependent control, are also examined. Chapter five lists some basic conclusions about solar sail escape trajectories. The computer program, as described in Appendix D, was the main tool for the analysis of solar sail escape trajectories.

2. FORCE MODEL

2.1 General Force Model

The intensity of sunlight can be expressed mathematically as follows (ref 6):

$$P_s = \int_0^{\infty} h \nu \eta(\nu) d\nu$$

where

P_s - solar intensity (watt/m²)

h - Plank's constant (joule-sec)

ν - frequency of a photon (1/sec)

$\eta(\nu)$ - number of photons per unit area per unit time per unit frequency (1/m²)

Experimentally this can be expressed as (ref 5):

$$P_s = 1353.9 \left[\frac{R_\odot}{R} \right]^2$$

where

R_\odot - mean radius of Earth's orbit = 1 a.u. = 1.495×10^{11} m

R - distance to the Sun (m)

The solar pressure, p , can then be determined as:

$$p = \frac{P_s}{c} = 4.513 \times 10^{-6} \left[\frac{R_\odot}{R} \right]^2 \quad (1)$$

where

p - solar pressure (newton/m²)

c - velocity of light = 3×10^8 m/sec

The characteristics of a reflecting surface may be defined in terms of the following parameters:

r - reflectivity of surface

a - absorption of surface

γ - transmissivity of surface

s - specular reflection coefficient

ϵ_f, ϵ_b - emissivity of the front and back surface

β_f, β_b - non-Lambertian coefficients, front and back surface

where $r+a+\gamma=1$. Since $\gamma=0$ for the solar sail's reflecting surface, $a=1-r$.

When light strikes a surface, three types of forces are created due to absorption, reflection and re-radiation of photons. The total force can be expressed as (ref 6):

$$\underline{F} = \underline{F}_R + \underline{F}_a + \underline{F}_r$$

where

\underline{F} - total force (newtons)

\underline{F}_R - force due to reflected photons (newtons)

\underline{F}_a - force due to absorbed photons (newtons)

\underline{F}_r - force due to re-radiated photons (newtons)

By defining the unit vectors \underline{i}' , \underline{n} , $\underline{\gamma}$, and \underline{m} as in figure 1, the following relations are obtained:

$$\underline{i}' = \cos\alpha \underline{m} + \sin\alpha \underline{\gamma}$$

$$\underline{m} = -\cos\alpha \underline{m} + \sin\alpha \underline{\gamma} = \underline{i}' - 2\cos\alpha \underline{m}$$

$$\underline{A} = \underline{A} \underline{n}$$

$$\underline{p} = p \underline{i}'$$

where A is the area of the sail and p is the solar pressure.

Since it may be assumed that all incident photons are initially absorbed by the reflector, \underline{F}_a can be expressed as

$$\underline{F}_a = (\underline{p} \cdot \underline{A}) \underline{i}' = p A \cos\alpha \underline{i}'$$

$$\underline{F}_a = p A (\cos^2 \alpha \underline{m} + \cos\alpha \sin\alpha \underline{\gamma}) \quad (2)$$

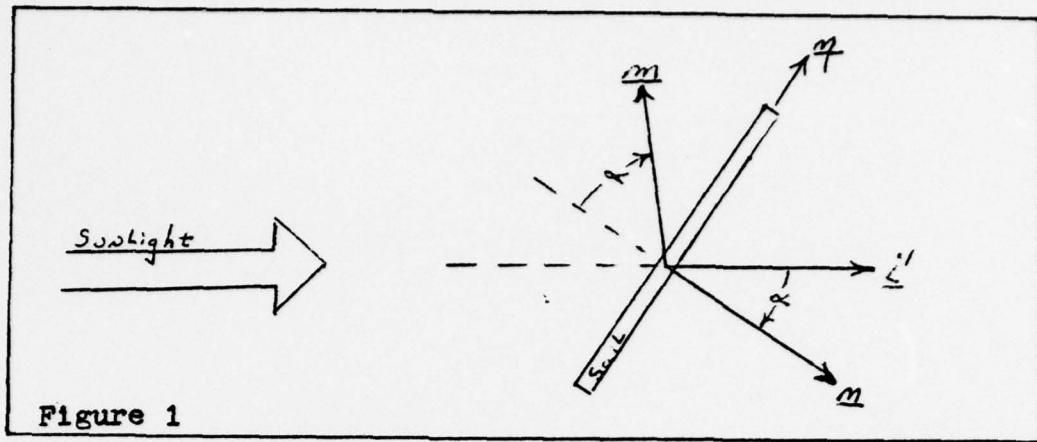


Figure 1

The force due to reflected photons is composed of two parts, due to specular (F_s) and non-specular (F_{ns}) reflection. The specularly reflected light causes a force in the $-m$ direction. This is expressed as

$$F_s = -(r_s)(\rho \cdot A) m$$

The non-specularly reflected light can be thought of as uniformly distributed over a hemisphere on the reflected side (see figure 2). The net flux will be in the $-n$ direction, thereby causing a force in the direction of n . The total non-specularly reflected hemispheric power is given by $c(1-s)r(\rho \cdot A)$. Assuming that Lambert's Law applies and using B_f to indicate that the sail's surface is not an ideal Lambertian surface, the force due to non-specularly reflected light can be expressed as (ref 6):

$$F_{ns} = B_f (1-s) r (\rho \cdot A) m$$

Combining the above expressions, the following equation for F_R can be obtained:

$$F_R = (\rho \cdot A) \left[B_f (1-s) r m - r s m \right]$$

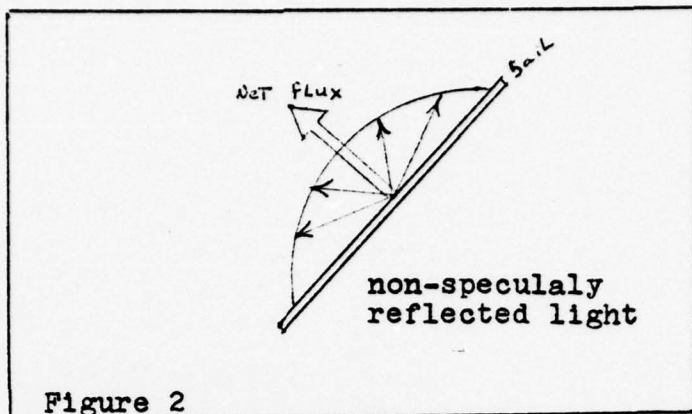


Figure 2

$$F_r = \rho A \left[(rs \cos^2 \alpha + B_f (1-s) r \cos \alpha) n - rs \cos \alpha \sin \gamma \right] \quad (3)$$

The power emitted from a unit area of a surface is given by $\epsilon \sigma T^4$ where ϵ is the emissivity of the surface, σ is the Stefan-Boltzman constant, and T is the temperature of the surface. Lambert's Law states that the force per unit area due to thermal re-radiation on an ideal Lambertian surface is $-\frac{2}{3} \frac{\epsilon \sigma T^4}{c} n$, where n is the outward normal of the surface. Using B_f and B_B to indicate that the solar sail is not an ideal Lambertian surface, the following expression for F_r can be obtained:

$$F_r = \frac{\sigma T^4}{c} (B_f \epsilon_f - B_B \epsilon_B) n$$

Figure 3 shows a small area of the sail that is in a steady state condition. Since the power in has to equal the power out, the following expression can be obtained (ref 6):

$$\sigma P A \cos \alpha = (\epsilon_f + \epsilon_B) \sigma T^4$$

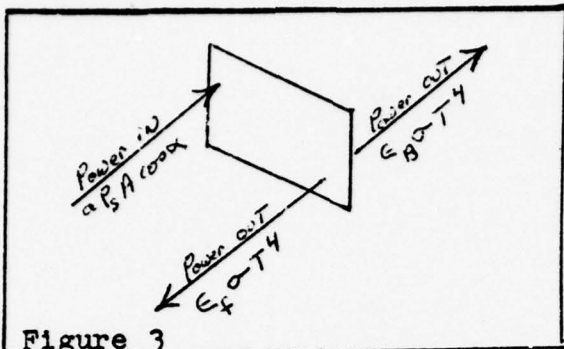


Figure 3

Dividing each side of the equation by c and rearranging terms:

$$\frac{\sigma T^4}{c} = \frac{(1-r) \rho A \cos \alpha}{(\epsilon_f + \epsilon_B)} \quad (4)$$

Substitution of this result into the expression for F_r gives:

$$F_r = \rho A (1-r) \frac{\epsilon_f \epsilon_f - \epsilon_B \epsilon_B}{(\epsilon_f + \epsilon_B)} \cos \alpha m \quad (5)$$

Equation 5 gives the impression that it would be best to build a solar sail with a low ϵ_B . Upon inspection of equation 4, one realizes that ϵ_B is the only parameter a designer has for regulation of the temperature of the sail, since the characteristics of the front side will probably be fixed such that maximum reflection occurs.

Combining equations 2, 3, and 5 gives the following general force model:

$$F = \rho A \left\{ \left[(1+r_s) \cos^2 \alpha + \epsilon_f (1-s) r \cos \alpha + (1-r) \left(\frac{\epsilon_f \epsilon_f - \epsilon_B \epsilon_B}{\epsilon_f + \epsilon_B} \right) \cos \alpha \right] m + \left[(1-r_s) \cos \alpha \sin \alpha \right] \eta \right\} \quad (6)$$

For a perfect reflector $r=1$, $s=1$, and $a=0$; therefore equation 6 reduces to

$$\underline{F} = 2\rho A \cos^2 \alpha \underline{m} \quad (7)$$

Equation 6 was derived assuming a flat sail with area A. A similar differential force model could be obtained. It must also be remembered, with reference to equation 6, that all of the sail's surface characteristics are functions of the temperature of the sail, the frequency of the radiation, and the surface material used. If the operating point is fairly constant, these values can be approximated by constants.

2.2 JPL Force Model

The Jet Propulsion Laboratory, using a differential form of equation 6, integrated the force over the surface of a sail which may be used for future missions. Angles θ and ϕ were defined as shown in figure 4. The incident angle α was varied and a curve fit was performed on the data. The force on the sail can be expressed as:

$$\underline{F} = F_f \underline{f}$$

where

F - force function magnitude(newtons)

f - unit vector in the direction of thrust vector

The force function magnitude can be expressed as(ref 16):

$$F = F_0 (c_1 + c_2 \cos 2\theta + c_3 \cos 4\theta) \quad (8)$$

where

$$F_0 = \rho A$$

θ - cone angle of the thrust vector with respect to the Sun-spacecraft line.

c_1, c_2, c_3 - sail force equation constants

From figure 4 the following expression can be obtained:

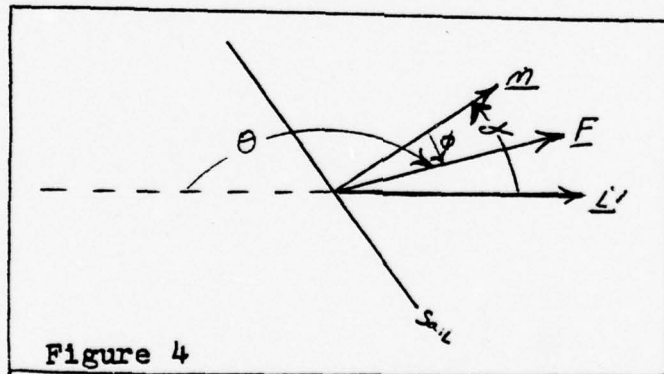
$$\alpha = 180^\circ - \theta + \phi$$

where

ϕ - cenerline angle, i.e. the angle between the surface normal and the thrust vector, measured in the direction from \underline{n} to \underline{i}' .

α - incident angle as defined in figure 1

A relationship exists between θ and ϕ , which is shown graphically in Appendix A, along with a plot of equation 8. If a certain θ is desired, the relationship between θ and ϕ is used to obtain ϕ , thereby determining α . Knowing α , the direction of the normal of the sail is fixed. The vectors \underline{i}' , \underline{F} , and \underline{n} are all in the same plane.



A perfect reflecting sail would be represented as:

$$F = F_0 (0.5 + 0.5 \cos 2\theta) \quad (9)$$

This is equivalent to equation 7.

Equation 8 will be called the JPL reflector and equation 9 will be called the perfect reflector.

The direction of the force function can be represented as:

$$f = \cos \theta \mathbf{i} + \sin \theta \sin \psi \mathbf{j} + \sin \theta \cos \psi \mathbf{k} \quad (10)$$

where the cone angle(θ) and clock angle(ψ) are defined in figure 5.

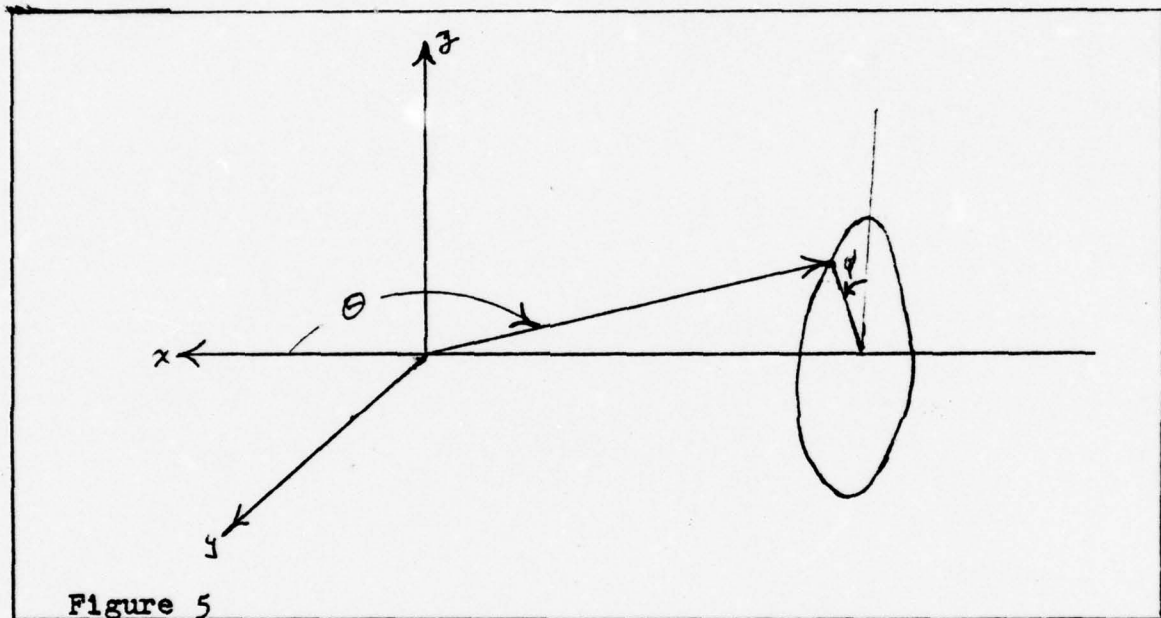


Figure 5

In order to compare the performance of different sails, a term a_c , the characteristic acceleration, is defined as follows:

$$a_c = \frac{F_0}{m_s}$$

Therefore the acceleration of the sail is

$$a_s = a_c (c_1 + c_2 \cos 2\theta + c_3 \cos 4\theta)$$

where

a_c - acceleration (m/sec^2)

m_s - total mass of solar sail vehicle (kg)

$$a_o = \frac{F_o}{m_s} = \frac{PA}{m_s} = 4.513 \times 10^{-6} \frac{A}{m_s} \left(\frac{R_\odot}{R} \right)^2 m/sec^2$$

Therefore

$$a_c = a_o (C_1 + C_2 \cos 2B + C_3 \cos 4B) f \quad (11)$$

The maximum variation of a_o due to variation of R (see definition above) at the sphere of influence of Earth is approximately 1%. Since this paper is concerned with Earth escape maneuvers that are well within the sphere of influence of Earth, it is reasonable to assume a_o constant over the maneuver.

2.3 Effects of Solar Wind and Earth Shine

The only force acting on the solar sail has been assumed to be the force due to solar radiation pressure. Other forces that might be considered are the forces from solar wind and Earth shine.

The solar wind intensity has been experimentally determined as follows (ref 5):

$$P_{sw} = 5 \times 10^{-2} \left[\frac{R_\odot}{R} \right]^2$$

The intensity of P_{sw} can increase by two or three orders of magnitude during periods of solar activity. Comparing P_{sw} and P_\odot it is evident that solar wind pressure is at least three to four orders of magnitude less than photon pressure. Solar wind will be neglected in this thesis. The major effect of solar wind is to deteriorate the sail's surface and thereby decrease the reflectivity.

To determine the effects of Earth shine an argument similar to the one developed in Villers (ref 15) is presented. The absorption of sunlight energy by the Earth is given as:

$$E_a = P_s \pi R_e^2 (1 - r_e)$$

where

E_a - power absorbed by the Earth (watts)

R_e - radius of the Earth (6378.16×10^3 m)

r_e - albedo/reflectivity of the Earth (.32 to .52)

P_s - solar intensity (watt/m²)

Assuming that all Earth shine effects occur at the Earth's surface and that the Earth re-radiates isotropically:

$$E_a = E_{RE} = P_{RE} (4\pi R_e^2)$$

where

E_{RE} - sunlight power re-radiated from Earth (watt)

P_{RE} - Earth re-radiated intensity at the Earth's surface (watt/m²)

substitution gives

$$P_{RE} = P_s \left(\frac{1 - r_e}{4} \right)$$

The maximum possible Earth shine intensity (P_{es}) is then

$$(P_{es})_{max} = P_{RE} + r_e P_s$$

$$(P_{es})_{max} = P_s \left(\frac{1 + 3r_e}{4} \right)$$

At a distance D above the Earth's surface the energy received from Earth shine has to be less than or equal to the maximum power emitted at the Earth's surface.

$$(E_{es})_{R_e + D} \leq \left[(E_{es})_{max} \right]_{R_e}$$

$$4\pi (R_e + D)^2 P_{es} \leq 4\pi R_e^2 (P_{es})_{max}$$

$$P_{es} \leq \left(\frac{R_e}{R_e + D}\right)^2 P_s \left(\frac{1 + 3R_e}{4}\right) \quad (12)$$

This paper assumes an operating point of at least 10 Earth radii. The effects of P_{es} will be at least two orders of magnitude less than P_s , and therefore will be neglected.

3. OPTIMIZATION

3.1 Coordinate Systems

An inertial coordinate system(*i*) and a rotating coordinate system(*R*) are defined as in figure 6 with the following assumptions and definitions:

1. Launch occurs at $t=0$.
2. The inertial and rotating coordinate system are centered at Earth with the x , y axes in the ecliptic plane and the z axis perpendicular to the ecliptic.
3. At $t=0$, the x axis of the inertial coordinate frame points at the Sun and remains fixed with respect to inertial space throughout the mission.
4. The rotating coordinate system has its x axis pointing at the Sun through out the mission.
5. Earth's orbit about the Sun is circular.
6. The difference between the Sun-spacecraft distance and the Sun-Earth distance is negligible.

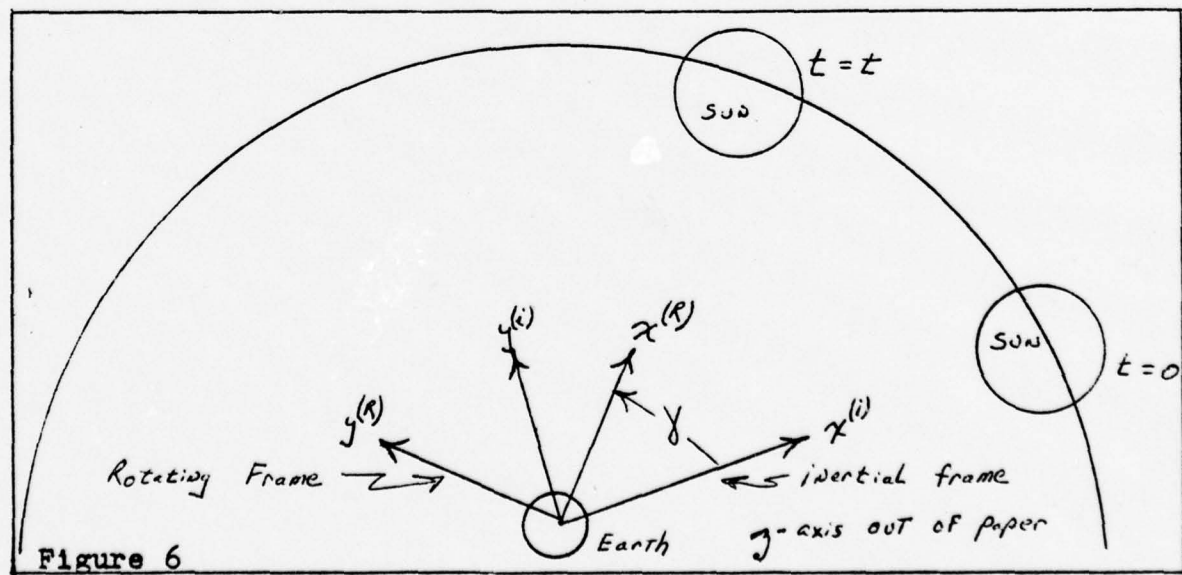


Figure 6

The angle γ as defined in figure 6 can be expressed as:

$$\gamma = \omega t \quad (13)$$

where

γ - angle of Sun with respect to the inertial coordinate frame (rad)

ω - rotation rate of Earth about the Sun ($1.9913859 \times 10^{-7} \frac{\text{rad}}{\text{sec}}$)

t - time (sec)

A rotation matrix that transforms the mathematical representation of a vector in the R frame to its equivalent vector representation in the I frame can be defined as:

$$C_R^i = \begin{bmatrix} \cos \gamma & -\sin \gamma & 0 \\ \sin \gamma & \cos \gamma & 0 \\ 0 & 0 & 1 \end{bmatrix} \quad (14)$$

3.2 Constraints

The accelerations on the solar sail are caused by gravity and solar pressure. The differential equations of motion can be written as:

$$\dot{\underline{r}}^{(i)} = \underline{v}^{(i)} \quad (15a)$$

$$\dot{\underline{v}}^{(i)} = \underline{a}_c^{(i)} - \frac{\mu}{r^3} \underline{r}^{(i)} \quad (15b)$$

where

μ - Earth's gravitational constant ($398601.2 \text{ km}^3/\text{sec}^2$)

$\underline{v}^{(i)}$ - velocity vector (km/sec)

$\underline{r}^{(i)}$ - radius vector (km)

$\underline{a}_c^{(i)} = a_c \underline{e}_f^{(i)} = a_c C_R^i \underline{e}_f^{(R)} \quad (\text{km/sec}^2)$

The solar sail has as control variables the cone and clock angles (θ and ψ) of the vector $\vec{f}^{(R)}$. The clock angle is unconstrained. The cone angle is constrained to be between θ_L and 180 degrees. The upper constraint on θ results from the mathematical definition of θ and ψ . The lower constraint results from the fact that the force vector can never point towards the Sun. The quantity θ_L is the limiting cone angle. For the perfect reflector, it is 90 degrees and for the JPL reflector it is the solution of the following equation:

$$C_1 + C_2 \cos 2\theta_L + C_3 \cos 4\theta_L = 0$$

this reduces to the following:

$$\cos \theta_L = - \sqrt{\frac{4C_3 - C_2 + \sqrt{C_2^2 + 8C_3^2 - 8C_1C_3}}{8C_3}} \quad (16)$$

Therefore the constraints on the control variables are:

$$\theta_L \leq \theta \leq 180^\circ \quad (17)$$

For the JPL square sail as given in Appendix A, θ_L is equal to 118.851 degrees.

3.3 The Optimal Control Law

Since the solar sail extracts energy from a limitless source for propulsion and attitude control, a performance index for trajectory optimization should not involve the energy source. There is an inherent assumption that the control law developed does not require changes in the control variables in a period of time that cannot be provided for by the attitude control system of the solar sail. The performance index J is given by:

$$J = \int_0^{\xi_f} (U) dt = \xi_f \quad (18)$$

The final objective of the maneuver is to achieve escape.

Therefore the final energy (E_f) has to equal zero.

$$E_f = \left[\frac{\underline{V}^{(i)T} \underline{V}^{(i)}}{2} - \frac{\mu}{(\underline{r}^{(i)T} \underline{r}^{(i)})^{1/2}} \right]_{t=t_f} = 0 \quad (19)$$

It is also assumed that the state (\underline{r} and \underline{V}) is given at $t=0$. This can be written as:

$$\underline{r}^{(i)0} = \underline{r}_0 \quad (20a)$$

$$\underline{V}^{(i)0} = \underline{V}_0 \quad (20b)$$

The problem is then to minimize J subject to the boundary conditions in equations 19 and 20 and the constraints in equations 15 and 17. The method used to achieve this optimization is to define a Hamiltonian which must be maximized in order to minimize J .

The Hamiltonian is defined as:

$$H = -1 + \underline{\lambda}_r^{(i)T} \underline{V}^{(i)} + \underline{\lambda}_v^{(i)T} \cdot \underline{a}_c^{(i)} + \underline{\lambda}_v^{(i)T} \cdot \underline{g}^{(i)} \quad (21)$$

where

H - Hamiltonian

$$\underline{g}^{(i)} = \frac{-\mu \underline{r}^{(i)}}{r^3} \quad (\text{km/sec}^2)$$

$\underline{\lambda}^{(i)}$ - position co-state vector with respect to inertial space (sec/km)

$\underline{\lambda}_v^{(i)}$ - velocity co-state vector (also called primer vector) with respect to inertial space (sec²/km)

Applying the Euler-Lagrange equations:

$$\frac{\partial H}{\partial \underline{V}^{(i)}} = - \underline{\lambda}_v^{(i)T}$$

therefore

$$\dot{\underline{\lambda}}_r^{(i)} = - \dot{\underline{\lambda}}_v^{(i)}$$

$$\frac{\partial H}{\partial \underline{r}^{(i)}} = - \dot{\underline{\lambda}}_r^{(i)T}$$

therefore

$$\dot{\underline{\lambda}}_r^{(i)} = \mu \frac{2}{\partial \underline{r}^{(i)}} \left[\frac{\underline{r}^{(i)T} \cdot \dot{\underline{\lambda}}_v^{(i)}}{(\underline{r}^{(i)T} \cdot \underline{r}^{(i)})^{3/2}} \right] = \mu \left[\frac{\dot{\underline{\lambda}}_v^{(i)}}{r^3} - \frac{3 \dot{\underline{\lambda}}_v^{(i)T} \cdot \underline{r}^{(i)}}{r^5} \underline{r}^{(i)} \right]$$

combining and rearranging terms gives:

$$\dot{\underline{\lambda}}_r^{(i)} = \frac{\mu}{r^3} \dot{\underline{\lambda}}_v^{(i)} - \frac{3\mu}{r^5} (\dot{\underline{\lambda}}_v^{(i)T} \cdot \underline{r}^{(i)}) \underline{r}^{(i)} \quad (22a)$$

$$\dot{\underline{\lambda}}_v^{(i)} = - \dot{\underline{\lambda}}_r^{(i)} \quad (22b)$$

Equations 22a and 22b are the co-state differential equations, whereas equations 15a and 15b are the state differential equations.

The force vector and primer vector directions can be represented as (see figure 7):

$$\underline{f}^{(R)} = \begin{bmatrix} \cos \theta \\ \sin \theta \sin \psi \\ \sin \theta \cos \psi \end{bmatrix} \quad (23a)$$

$$\frac{\dot{\underline{\lambda}}_v^{(R)}}{\dot{\underline{\lambda}}_v} = \begin{bmatrix} \cos \beta \\ \sin \beta \sin \sigma \\ \sin \beta \cos \sigma \end{bmatrix} \quad (23b)$$

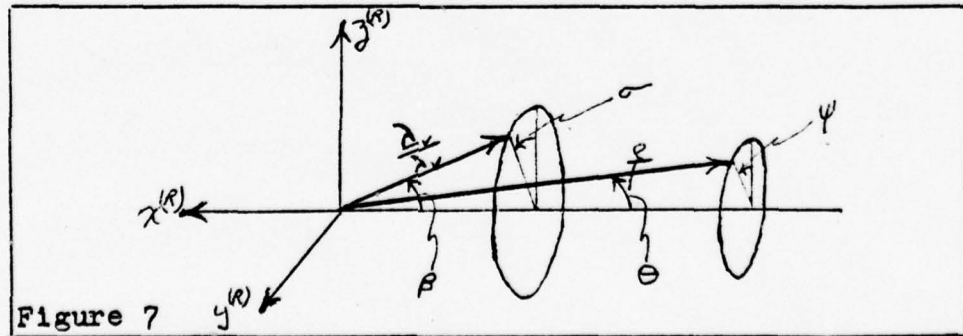


Figure 7

Since the control variable ψ has no constraints, the Hamiltonian can be maximized with respect to ψ by setting the partial of the Hamiltonian with respect to ψ equal to zero. The Hamiltonian of concern is:

$$\begin{aligned}
 H' &= \underline{\lambda}_v^{(i)T} \cdot \underline{a}_c^{(i)} = \underline{\lambda}_v^{(i)T} \cdot \left[a_c C_R^i \underline{f}^{(R)} \right] \\
 &= a_c \left[\underline{\lambda}_v^{(i)T} C_R^i \right] \cdot \underline{f}^{(R)} = a_c \underline{\lambda}_v^{(R)T} \cdot \underline{f}^{(R)} \\
 &= a_c \lambda_v \left[\cos \theta \cos \beta + \sin \theta \sin \beta (\sin \psi \sin \sigma + \cos \psi \cos \sigma) \right] \\
 \frac{\partial H'}{\partial \psi} &= 0 = a_c \lambda_v \sin \theta \sin \beta (\sin \sigma \cos \psi - \sin \psi \cos \sigma)
 \end{aligned}$$

$$\therefore \tan \psi = \tan \sigma$$

$$\psi = \sigma \quad (24)$$

From equation 24 it is evident that the force vector, the primer vector, and the x axis of the rotating coordinate frame will all be in the same plane. Therefore the force vector's direction can be expressed as (ref 12):

$$\underline{f}^{(R)} = \frac{\sin(\beta - \theta)}{\sin \beta} \begin{bmatrix} 1 \\ 0 \\ 0 \end{bmatrix} + \frac{\sin \theta}{\sin \beta} \left(\frac{\underline{\lambda}_v^{(R)}}{\lambda_v} \right)$$

$$\underline{f}^{(i)} = \frac{\sin(\beta - \theta)}{\sin \beta} C_R^i \begin{bmatrix} 1 \\ 0 \\ 0 \end{bmatrix} + \frac{\sin \theta}{\sin \beta} C_R^i \left(\frac{\underline{\lambda}_v^{(R)}}{\lambda_v} \right)$$

$$\dot{\varphi}^{(i)} = \frac{\sin(\beta - \theta)}{\sin \beta} \begin{bmatrix} \cos \gamma \\ \sin \gamma \\ 0 \end{bmatrix} + \frac{\sin \theta}{\sin \beta} \begin{bmatrix} \frac{\lambda^{(i)}}{\lambda_v} \\ \lambda_v \end{bmatrix} \quad (25)$$

Because the control variable ϵ is constrained as expressed in equation 17, the Maximum Principle must be applied in the determination of the control law for θ . Substitution of equation 24 into the expression for the Hamiltonian and rearranging terms gives the following Hamiltonian of concern:

$$H' = (a_c \lambda_v) [\cos(\theta - \beta)]$$

For the ideal reflector:

$$a_c = a_0 \cos^2 \theta$$

$$\frac{\partial H'}{\partial \theta} = 0 = -2 \cos \theta \sin \theta \cos(\theta - \beta) + \cos^2 \theta [-\sin \theta \cos \beta + \cos \theta \sin \beta]$$

$$2 \sin \beta \tan^2 \theta + 3 \cos \beta \tan \theta - \sin \beta = 0$$

therefore

$$\tan \theta = \frac{-3 \cos \beta \pm \sqrt{9 \cos^2 \beta + 8 \sin^2 \beta}}{4 \sin \beta}$$

The ambiguity of the sign in the above equation is removed by use of the necessary condition that the second partial of H' with respect to θ has to be less than zero at a point that maximizes H' . Substitution of the above value of θ into $\frac{\partial^2 H'}{\partial \theta^2}$ yields:

$$- \cos^3 \theta \sec^2 \theta \left[\pm \sqrt{9 \cos^2 \beta + 8 \sin^2 \beta} \right] < 0$$

Since θ is in the second quadrant, the sign of the radical has to be negative. This same result would have been achieved if physical reasoning were used to remove the ambiguity of the above sign. If the sign was positive, $\tan \theta$ would be greater than zero and therefore θ would violate the constraint equation. Therefore the cone angle control law for a perfect reflector is:

$$\tan \theta = - \frac{3 \cos \beta + \sqrt{9 \cos^2 \beta + 8 \sin^2 \beta}}{4 \sin \beta} \quad (26a)$$

$$90^\circ \leq \theta \leq 180^\circ \quad (26b)$$

Proceeding in a similar manner for the JPL reflector, it is found that the equations do not solve analytically in closed form. A second order Newton iteration method can be used to solve for the optimal θ . The Hamiltonian of concern can be written as:

$$H' = D(\theta) E(\theta, \beta)$$

where

$$D(\theta) = C_1 + C_2 \cos 2\theta + C_3 \cos 4\theta$$

$$E(\theta, \beta) = \cos(\theta - \beta)$$

defining the following:

$$HP = \frac{\partial H'}{\partial \theta} = \left[\frac{\partial D(\theta)}{\partial \theta} \right] E(\theta, \beta) + D(\theta) \left[\frac{\partial E(\theta, \beta)}{\partial \theta} \right]$$

$$HPP = \frac{\partial^2 H'}{\partial \theta^2} = \left[\frac{\partial^2 D(\theta)}{\partial \theta^2} \right] E(\theta, \beta) + 2 \left[\frac{\partial D(\theta)}{\partial \theta} \right] \left[\frac{\partial E(\theta, \beta)}{\partial \theta} \right] + D(\theta) \left[\frac{\partial^2 E(\theta, \beta)}{\partial \theta^2} \right]$$

Therefore the optimal θ is given by:

$$\Theta^{(n+1)} = \Theta^{(n)} - \frac{HP(\Theta^{(n)})}{HPP(\Theta^{(n)})} \quad (27a)$$

$$\Theta^{(n)} \text{ is given by equation 26} \quad (27b)$$

$$\Theta_L \leq \Theta \leq 180^\circ \quad (\Theta_L \text{ is given in equation 16}) \quad (27c)$$

From equation 24 and 26, it is evident that expressions for β and σ must be obtained. From equation 23b the following expression for β can be obtained:

$$\cos \beta = \frac{\lambda_v^{(k)} \cdot \begin{bmatrix} 1 \\ 0 \\ 0 \end{bmatrix}}{|\lambda_v^{(k)}|} = \frac{\begin{bmatrix} \lambda_v^{(k)} & \lambda_v^{(k)} \end{bmatrix}^T \cdot \begin{bmatrix} 1 \\ 0 \\ 0 \end{bmatrix}}{|\lambda_v^{(k)}|}$$

therefore

$$\beta = \cos^{-1} \left[\frac{\cos \gamma (\lambda_{vx}^{(k)}) + \sin \gamma (\lambda_{vy}^{(k)})}{|\lambda_v^{(k)}|} \right] \quad (28)$$

where $\lambda_{vx}^{(k)}$ and $\lambda_{vy}^{(k)}$ are the x and y components of the primer vector with respect to the inertial coordinate frame.

In a similar manner it can be shown that:

$$\sigma = \tan^{-1} \left[\frac{\cos \gamma (\lambda_{vy}^{(k)}) - \sin \gamma (\lambda_{vx}^{(k)})}{\lambda_{vz}^{(k)}} \right] \quad (29)$$

From equations 26 and 27 it is clear that β must be determined before the optimal thrust cone angle (θ) can be determined. Since in this thesis the optimal θ will be determined and then checked to see if it is within the constraints, considerable work could be avoided if the constraints in equation 17 could

be expressed in terms of β . The optimal θ is obtained when the partial of the Hamiltonian with respect to θ (HP as defined above) is set equal to zero. If it is assumed that the situation is such that θ_L (and therefore $\beta = \beta_L$) is the optimal θ , the following would result:

$$D(\theta_L) \left[\frac{\partial E(\theta, \beta)}{\partial \theta} \right]_{\substack{\theta = \theta_L \\ \beta = \beta_L}} + \left[\frac{\partial D(\theta)}{\partial \theta} \right]_{\theta = \theta_L} E(\theta_L, \beta_L) = 0$$

$$D(\theta_L) = C_1 + C_2 \cos 2\theta_L + C_3 \cos 4\theta_L = 0$$

Since $\left[\frac{\partial D(\theta)}{\partial \theta} \right]_{\theta_L}$ is not equal to zero for all possible θ_L , it can be concluded that:

$$E(\theta_L, \beta_L) = \cos(\theta_L - \beta_L) = 0$$

Therefore

$$\beta_L = \theta_L - \frac{\pi}{2}$$

Upon inspection of equation 26 it is realized that as β approaches 180 degrees, θ approaches 180 degrees. Therefore the constraints imposed upon θ in equation 17 can be replaced by the following:

$$\theta_L - \frac{\pi}{2} \leq \beta \leq 180^\circ \quad (30)$$

3.4 Boundary Conditions

The boundary conditions are now addressed. This thesis assumes that the state is completely described at launch as given in equation 20. Boundary conditions on the co-state must

now be determined based upon equation 19.

From Appendix B the following conditions on the co-state must exist at the final time:

$$\dot{\underline{\Delta}}_f^{(i)} = - \left[\frac{\partial S}{\partial \underline{\underline{\chi}}^{(i)}} + \underline{\mathcal{L}}^T \frac{\partial \underline{\Psi}^{(i)}}{\partial \underline{\underline{\chi}}^{(i)}} \right]_{t=t_f}^T \quad (31a)$$

$$\left[\frac{\partial S}{\partial t} + \underline{\mathcal{L}}^T \frac{\partial \underline{\Psi}^{(i)}}{\partial t} + L + \left(\frac{\partial S}{\partial \underline{\underline{\chi}}^{(i)}} + \underline{\mathcal{L}}^T \frac{\partial \underline{\Psi}^{(i)}}{\partial \underline{\underline{\chi}}^{(i)}} \right) \cdot \dot{\underline{\underline{\chi}}}^{(i)} \right]_{t=t_f} = 0 \quad (31b)$$

$$\underline{\Psi}^{(i)}(\underline{\underline{\chi}}^{(i)}, t_f) = 0 \quad (31c)$$

For the solar sail escape maneuver, the following terms can be identified:

$$S = 0$$

$$L = 1$$

$$\underline{\Psi}^{(i)} = \left[\frac{\sqrt{\underline{\underline{\chi}}^{(i)} \cdot \underline{\underline{V}}^{(i)}}}{2} - \frac{\underline{\mathcal{L}}}{(\underline{\underline{r}}^{(i)T} \cdot \underline{\underline{r}}^{(i)})^{1/2}} \right]_{1 \times 1}$$

$$\underline{\mathcal{L}} = [\underline{\mathcal{L}}]_{1 \times 1}$$

$$\underline{\underline{\chi}}^{(i)} = \begin{bmatrix} \underline{\underline{r}}^{(i)} \\ \underline{\underline{V}}^{(i)} \end{bmatrix}$$

$$\underline{\underline{r}}^{(i)} = \begin{bmatrix} \underline{\underline{r}}^{(i)} \\ \underline{\underline{V}}^{(i)} \end{bmatrix}$$

Substitution of these terms into equations 31a and 31b and eliminating ν from the equations results in the following boundary conditions for the co-state:

$$\left(\dot{\lambda}_r^{(i)} \right)_{t=t_f} = \left[\frac{-\frac{q^{(i)}}{r}}{\sqrt{\mu^{(i)T} \cdot Q_c^{(i)}}} \right]_{t=t_f} \quad (32a)$$

$$\left(\dot{\lambda}_v^{(i)} \right)_{t=t_f} = \left[\frac{\sqrt{\frac{1}{\mu^{(i)T} \cdot Q_c^{(i)}}}}{r} \right]_{t=t_f} \quad (32b)$$

where

$$\frac{q^{(i)}}{r} = -\frac{\mu_r^{(i)}}{r^3}$$

The final time (t_f) can be obtained from equation 31c (equation 19).

3.5 Summary

The analysis of an optimal Earth escape maneuver to zero energy results in a two-point boundary value problem of a 12th order system. The implementation of the analysis in this thesis is to guess an initial co-state and then by use of a Runge-Kutta algorithm, integrate equations 15 and 22 until the energy equals zero. At each point of the integration the control law is determined by equations 24 and 27 in conjunction with equations 28 and 29. The final co-state is checked to see if it satisfies equation 32. If it does not (to a desired accuracy), an iteration scheme is developed that improves the initial guess of the co-state. This iteration is continued until the desired accuracy is achieved.

A Newton-Raphson iteration scheme was used to improve the initial guess of the co-state. A development of the Newton-Raphson iterator is presented in Appendix C. The computer program developed to implement the above analysis is presented in Appendix D.

4. DISCUSSION

4.1 Introduction

The purpose of this thesis is to develop the optimal control law necessary for a minimum time escape from a high Earth orbit with a solar sail. The end result is a computer program (see Appendix D) that determines the time history of the optimal control law. With minor changes, this computer program could be used to determine optimal escape trajectories from planets other than Earth.

The computer program developed does not have active constraints to prevent the optimal trajectory from going below a certain desired altitude. This was not a serious problem for escape trajectories whose initial orbit was above 100000 kilometers. Some escape trajectories from initial ecliptic orbits with a semi-major axis of 100000 kilometers or less did intersect the surface of the Earth. A recommended solution to this problem is to add a penalty function to the performance index which heavily penalizes trajectories close to the surface of the Earth.

A Newton-Raphson iteration scheme was used to solve the two-point boundary value problem. The computer program developed had problems converging for some initial orbits. The convergence problems were usually caused because the initial guess of the co-state was too far from the optimal initial co-state for the Newton-Raphson iterator to work. One possible solution to this problem is to develop a gradient method for solving the two-point boundary value problem with a velocity-dependent

control law (discussed below) as the initial guess. Another possible solution to this problem is to use the velocity-dependent control law to obtain an estimate of the optimal escape trajectory. Using equation 32 and the estimate of the optimal escape trajectory, an approximation to the final optimal co-state can then be obtained. The computer program in Appendix D can then be used to integrate the state and co-state backwards in time until the initial or near initial state is reached. The initial co-state as given by the backward integration will usually be sufficiently close to the optimal initial co-state such that a converged escape trajectory can be obtained. This latter method has proved successful in this thesis.

Although this thesis is concerned mainly with the optimal control law, two other sub-optimal control laws were examined. They are called open-loop control and velocity-dependent control.

An open-loop control trajectory results when equations 15 and 22 are integrated forward in time with the initial co-state vectors as given below:

$$\lambda_{r_0}^{(i)} = \frac{V_c}{|\Gamma_0^{(i)}|^2} \Gamma_0^{(i)} \quad (33a)$$

$$\lambda_{V_0}^{(i)} = \frac{V_0}{|V_c^{(i)}|} \quad (33b)$$

The quantities $\underline{r}_0^{(i)}$ and $\underline{V}_0^{(i)}$ are the initial state vectors with respect to the initial coordinate frame, and V_c is the circular orbital velocity associated with $\underline{r}_c^{(i)}$. At each point of the integration the control variables θ and ψ are determined by equations

24 and 27 in conjunction with equations 28 and 29. No attempt is made in open-loop control to satisfy equation 32. An open-loop control trajectory would be the optimal control trajectory if the initial guess of the co-state (equation 33) was the optimal initial co-state. Equation 33 results from the fact that tangential thrust has been shown to be a good approximation to the optimal thrust for initial circular orbits (ref 4).

Velocity-dependent control results when the acceleration vector (equation 11) is required to lie in the plane of the x axis of the rotating coordinate frame and the velocity vector and is oriented in the direction that maximizes its projection on the velocity vector. A velocity-dependent control trajectory results when equation 15 is integrated forward in time with ψ and θ being determined at each point of the integration by equations 24 and 27 in conjunction with σ and β as defined below:

$$\sigma = \tan^{-1} \left[\frac{(\cos \delta) V_y^{(i)} - (\sin \delta) V_x^{(i)}}{V_z^{(i)}} \right] \quad (34a)$$

$$\beta = \cos^{-1} \left[\frac{(\cos \delta) V_x^{(i)} + (\sin \delta) V_y^{(i)}}{|V^{(i)}|} \right] \quad (34b)$$

Satisfaction of the constraints in equation 17 is also required. Velocity-dependent control relies only upon the state, and therefore there is no need for the co-state equations and boundary conditions.

4.2 Optimal Control

Figures 8 and 9 are the time histories of the optimal

control variables for a minimum time escape from an initial 150000 kilometer circular ecliptic Earth orbit. The maximum rate of change of the control variable θ is approximately one degree per hour. The JPL square sail can sustain an attitude rate of between 20 to 25 degrees per hour. The infinite attitude rates of the control variable ψ results from the mathematical singularities associated with cone and clock angle representation. At 1.7 and 4.5 days θ is at 180 degrees and therefore ψ can have any value for the same force vector. Because the JPL square sail is not ideal, its θ_L , as given by equation 16, is not 90 degrees. This is indicated as a straight line between 5.9 and 9.1 days on figure 8. During this period ψ can be rotated through the necessary 180 degrees while θ is maintained at θ_L . This results in an attitude rate of about 2.5 degrees per hour. Similar results were obtained for initial 100000 kilometer circular ecliptic orbits with resulting attitude rates about twice as large. The attitude rates of the solar sail tend to be inversely proportional to the semi-major axis of the initial orbit.

Figure 10 demonstrates some of the basic characteristics of optimal escape trajectories from ecliptic orbits with a solar sail. The trajectory tends to become very eccentric quickly with the instantaneous semi-major axis of the trajectory perpendicular to the Sun-spacecraft line in the orbital plane. The instantaneous pericenter of the trajectory is on the side of the Earth on which the solar sail can achieve its maximum thrust in

the direction of the velocity vector. Figure 11 shows the increase in eccentricity for various initial ecliptic orbits.

The optimal control law for an initial orbit inclined to the ecliptic plane is shown in figure 12. The initial orbit considered is the initial circular ecliptic orbit in figure 10, rotated out of the ecliptic plane by 30 degrees. Symmetry about the x-z plane is maintained. The control law for θ is similar to figure 8. The time to escape is 0.1 days longer than that from a similar initial ecliptic orbit. The control law for ψ is less demanding, and the trajectory tends to become eccentric slower than it does for a similar initial ecliptic orbit. The instantaneous semi-major axis of the orbit is in the orbital plane perpendicular to the Sun-spacecraft line. As the inclination of the initial orbit is increased, the control law tends to be less demanding, and the escape time tends to be longer.

The optimal control law for an initial 150000 kilometer circular polar orbit is shown in figures 13 and 14. The control variable θ has a very low attitude rate. The attitude rate of ψ is about 2.2 degrees per hour at first and then falls off considerably. The optimal escape trajectory from circular polar orbits maintains a low eccentricity throughout most of the escape maneuver as shown in figure 15. Similar results were obtained for lower initial polar orbits. As can be seen, the attitude rates for initial polar orbits are less than those for similar initial ecliptic orbits but the final time is longer.

It appears that the performance of a solar sail will tend

to be between the limiting cases of the resulting escape trajectories from similar ecliptic and polar initial orbits. The ecliptic initial orbit will yield the highest attitude rates that can be expected and the smallest final escape time. The polar initial orbit will yield the lowest attitude rates and the largest final time.

4.3 Open-Loop Control

Open-loop control is, as the name implies, an open loop trajectory of the optimal control law with the initial guess of the co-state vectors as given in equation 33. For initial circular ecliptic orbits, open-loop control is a good approximation to the optimal control.

For the initial 150000 kilometer circular ecliptic orbit in figure 8, the final escape time predicted by open-loop control varies from the optimal control final escape time by less than 1%. For the initial 100000 kilometer circular ecliptic orbit in figure 11, the error is around 4%. As the eccentricity of the initial orbit is increased the error between open-loop and optimal control increases. For the initial eccentric ecliptic orbit in figure 11 (100000 kilometer pericenter, 0.25 eccentricity), the error in the final escape time between these two methods is about 8.5%. As the inclination of the initial orbit with respect to the ecliptic is increased, the error between optimal and open-loop control also increases. It can generally be concluded that the open-loop control law is a good approximation to the optimal control law for a minimum time escape from high

Earth orbits with low inclination and low eccentricity.

Figures 16a and 16b were constructed using open-loop control. Figure 16a shows the final escape time for four various starting positions from a 150000 km circular ecliptic orbit. Figure 16b shows how the energy increases during the escape maneuver of two of the trajectories considered in figure 16a. In figure 16b the sharp increases in energy followed by little or no increases is because in the ecliptic plane the solar sail increases its energy from solar radiation pressure only when it is traveling away from the Sun. From figure 16b it can be seen that the initial energy of the solar sail determines how much energy must be added in order to achieve escape. Given the initial energy, certain starting positions make it possible for the solar sail to achieve escape prior to making another revolution over that portion of the trajectory where the vehicle is traveling towards the Sun. This is the case for \sqrt{v} equal to 270 degrees in figure 16b. For \sqrt{v} equal to 90 degrees in figure 16b, the effects of having to traverse the "backside" of the trajectory an additional time in order to reach escape condition is obvious. It can also be seen that if the eccentricity of the orbit is changed, the initial energy and starting position remaining the same, the final escape time will be affected because the time in which the solar sail is in "useful" sunlight is changed. It therefore appears that the final escape time from ecliptic orbits is dependent not only upon the initial energy of the vehicle but also upon its starting position within the orbit and the eccentricity of the initial orbit.

4.4 Velocity-Dependent Control

The velocity-dependent control law orients the force vector of the sail in a direction that maximizes its projection on the velocity vector in the plane of the velocity vector and the Sun-spacecraft line while still satisfying equation 17. Velocity-dependent control is rather interesting in that it is simpler to implement and analyze and yet gives results that are close to optimal.

For the initial 150000 km circular ecliptic orbit in figure 8, velocity-dependent control yields a final time of 20.33 days. The optimal final escape time was 20.29 days, and the open-loop control law yielded a final time of 20.29 days. This gives an error of about 1.2% between velocity-dependent and optimal control. For the 100000 km circular ecliptic initial orbit in figure 11, the error in final time between velocity-dependent and optimal control was 1.7%. As the initial orbit is inclined to the ecliptic plane, the error between velocity-dependent and optimal control increases. For the initial 150000 km circular polar orbit in figures 13 and 14, the optimal escape trajectory gave an escape time of 29.45 days. The velocity-dependent control law yielded a final escape time of 30.42 days. This is an error of about 3.3% between velocity-dependent and optimal control. The open-loop control law gave a final escape time of 32.7 days which results in an error of 11% from the optimal control law.

The velocity-dependent control law was used to obtain figures 17a and 17b. Figure 17a shows that starting position in the ecliptic plane has little effect upon the final escape

time. Figure 17b shows that for a polar orbit the increase in energy is nearly uniform through out the escape maneuver. Therefore the final escape time from polar orbits is almost totally dependent upon the initial energy of the vehicle. Starting position in the orbit and the eccentricity of the initial orbit have little effect upon the escape time from polar orbits

The velocity-dependent control law appears to be a good approximation for the optimal control law of a minimum time escape from high Earth orbits. As the orbit is inclined the velocity-dependent control law is a better approximation to the optimal control law than open-loop control.

Optimal Control - Theta versus time

initial circular ecliptic orbit

$$\underline{r}_o^{(i)} = 150000 \text{ km } \underline{i}$$

$$\underline{v}_o^{(i)} = 1.63014 \text{ km/sec } \underline{j}$$

JPL square sail $a_o = 1 \text{ mm/sec}^2$

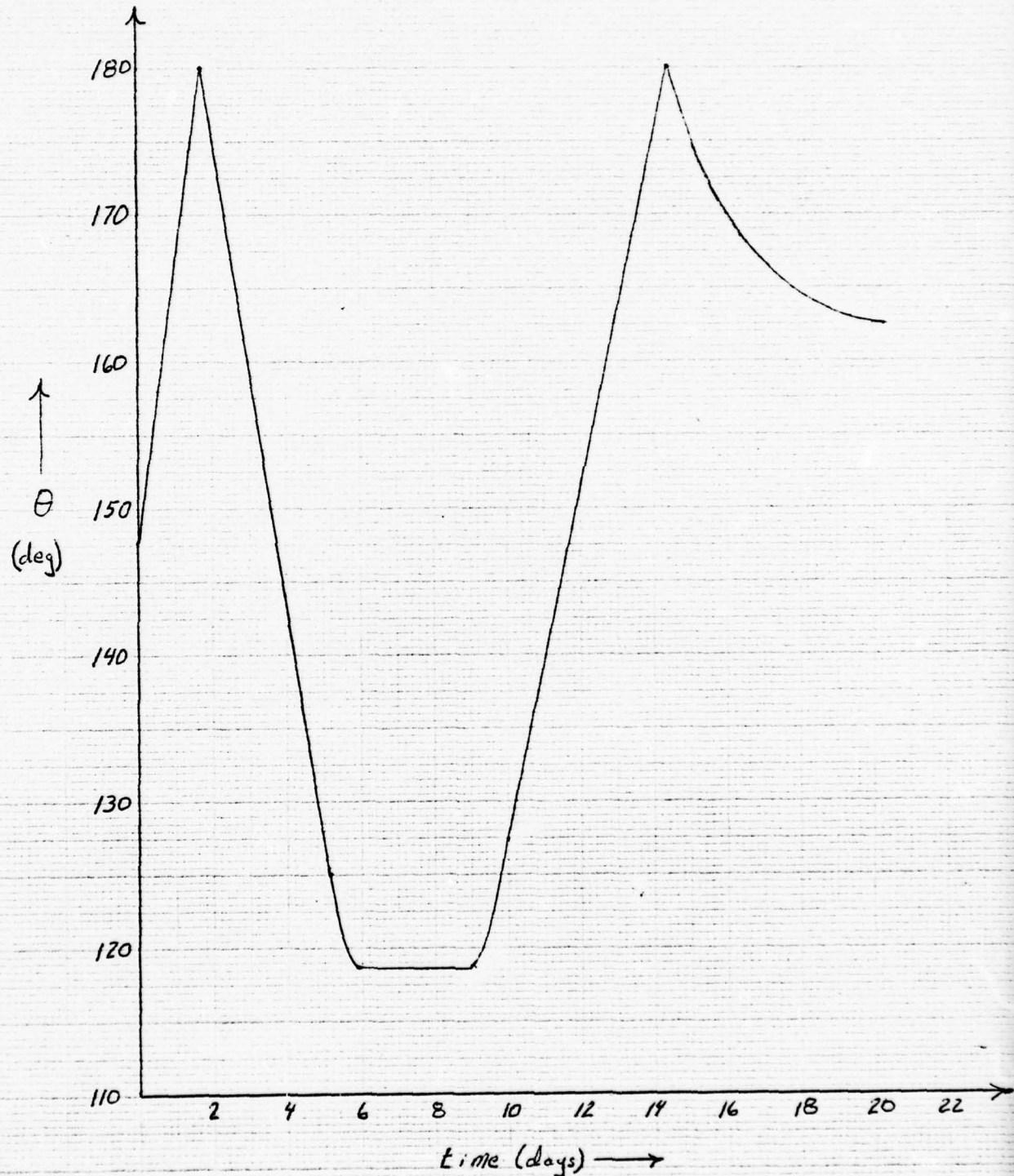


Figure 8

40a

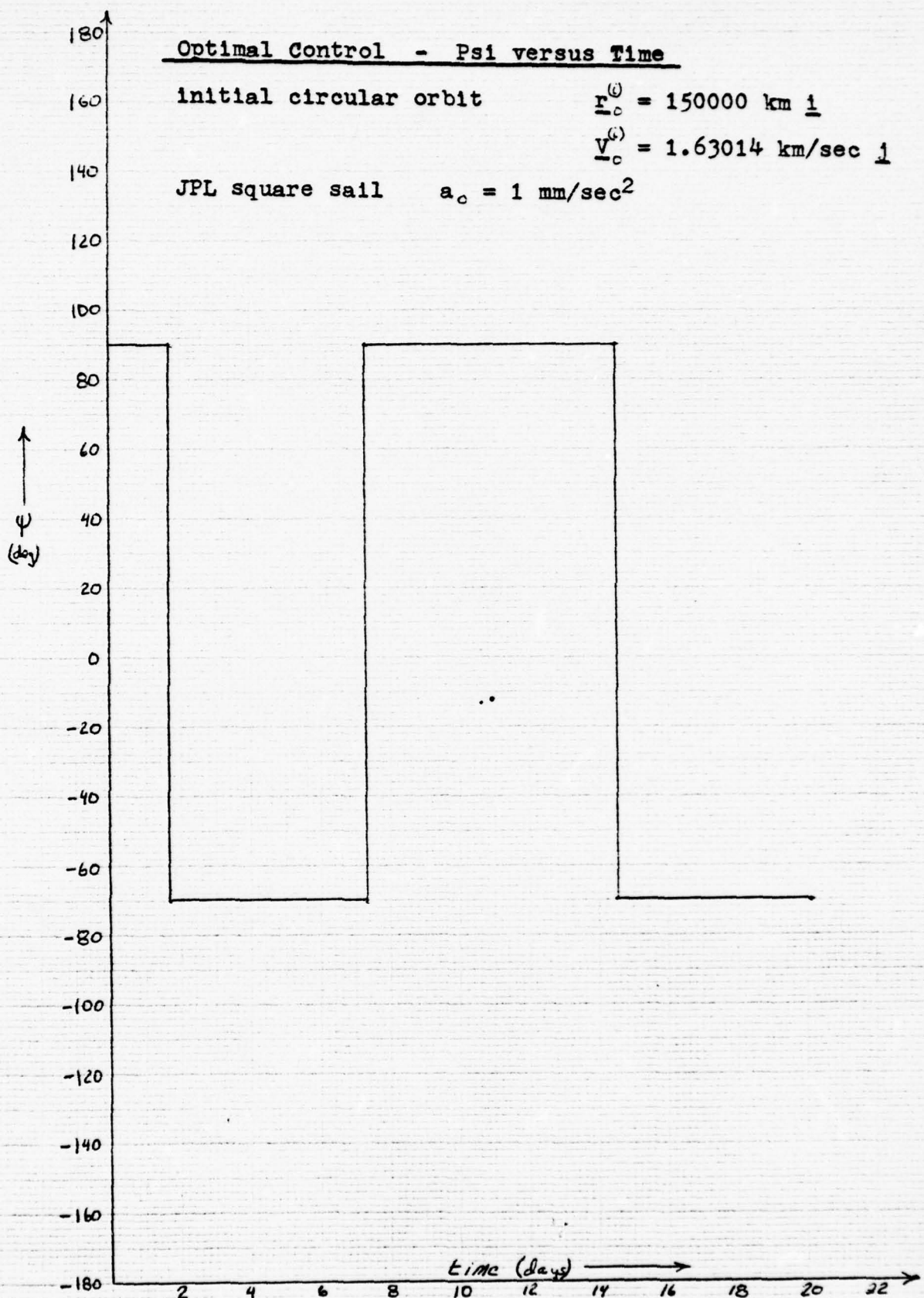


Figure 9

40b

JPL square sail
 $a_0 = 1 \text{ mm/sec}^2$

Optimal Escape Trajectory

initial circular ecliptic orbit

$$\underline{r}_0^{(i)} = 150000 \text{ km } \underline{1}$$

$$\underline{v}_0^{(i)} = 1.63014 \text{ km/sec } \underline{1}$$

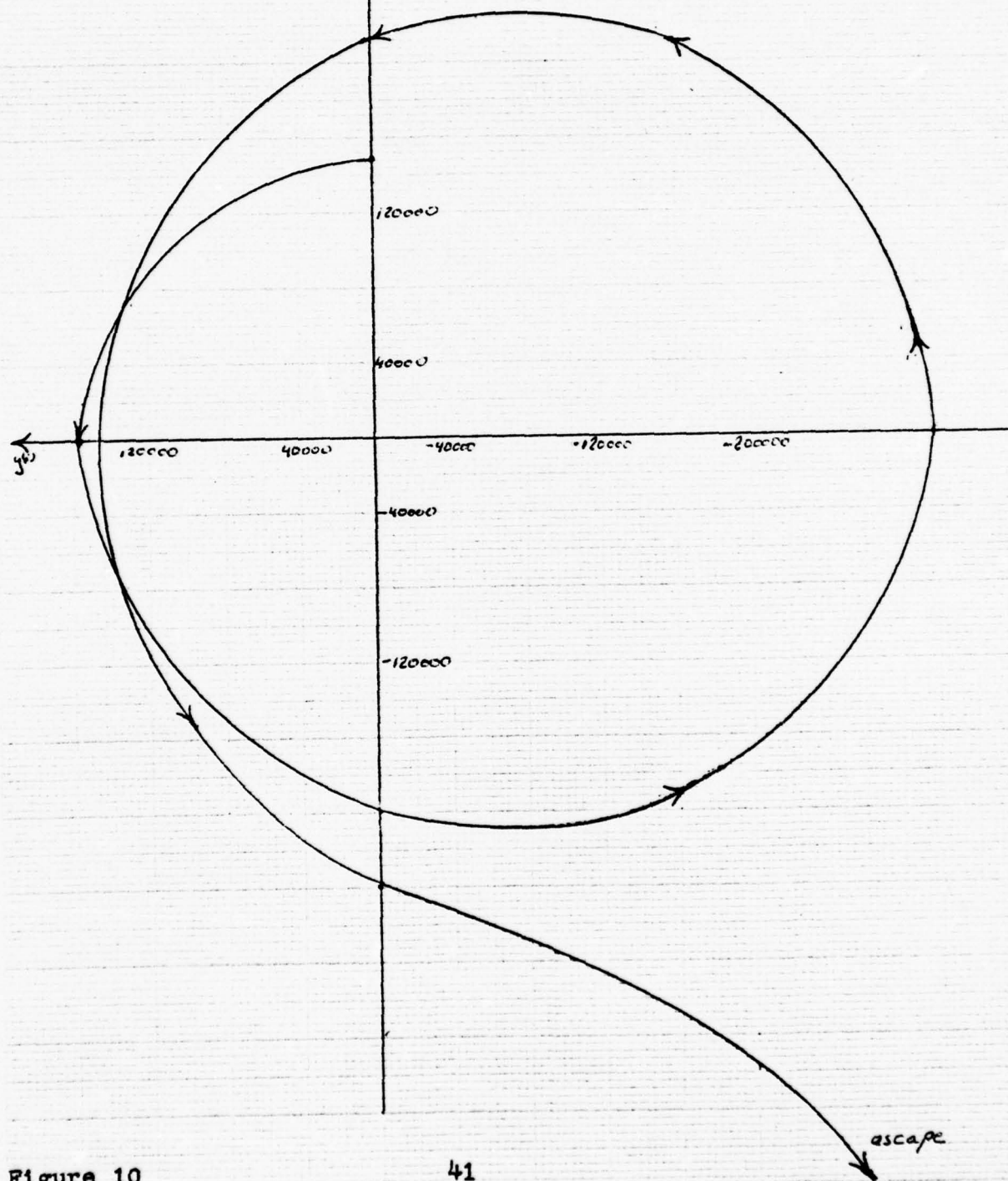


Figure 10

Eccentricity versus Time for various initial orbits - Optimal Control

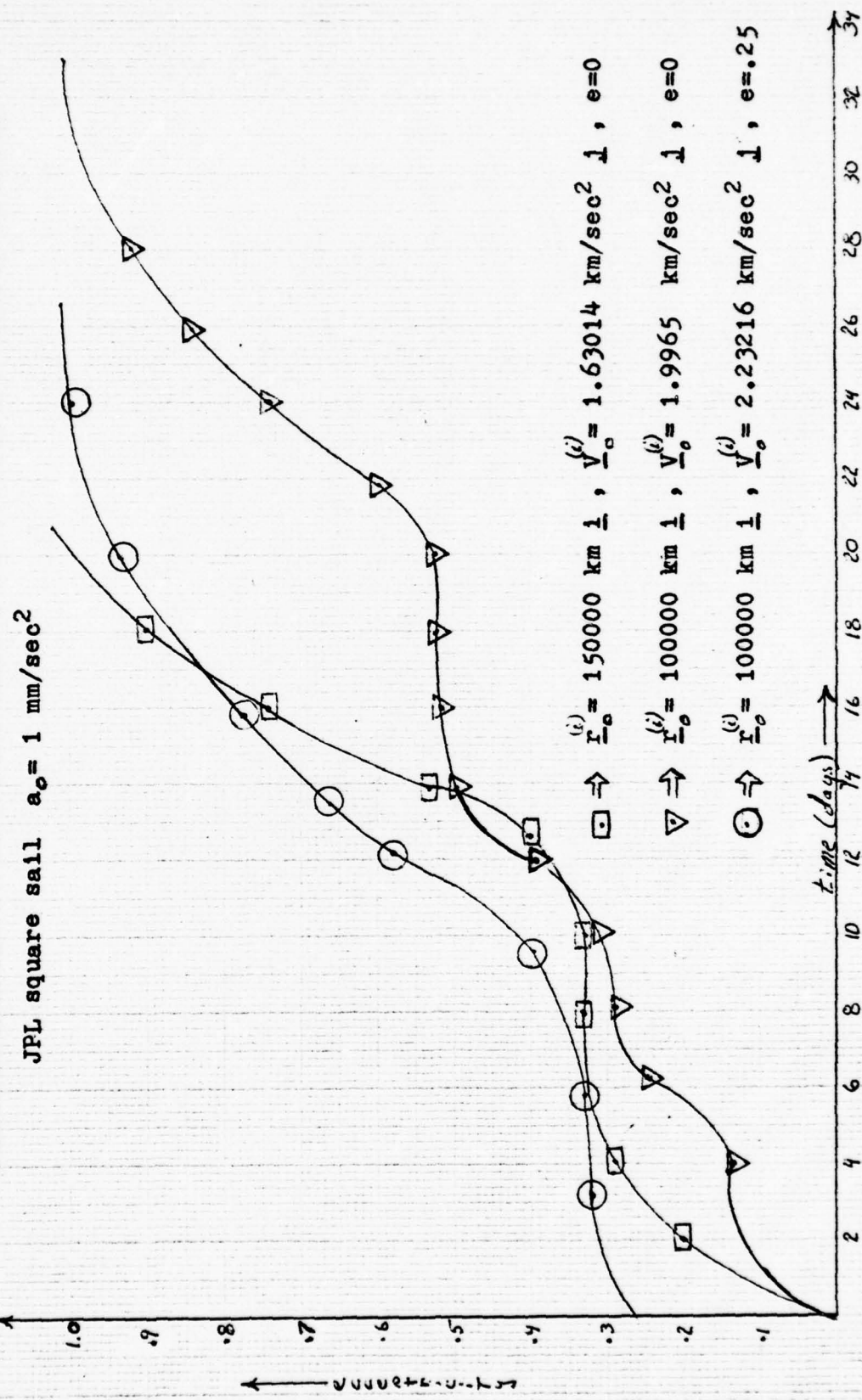


Figure 11

Optimal Control - Psi versus Time

initial circular inclined orbit

$$r_o^{(i)} = 150000 \text{ km } \underline{i}$$

$$v_o^{(i)} = 1.4117 \underline{i} + 0.81507 \underline{k} \text{ km/sec}$$

JPL square sail

$$a_s = 1 \text{ mm/sec}^2$$

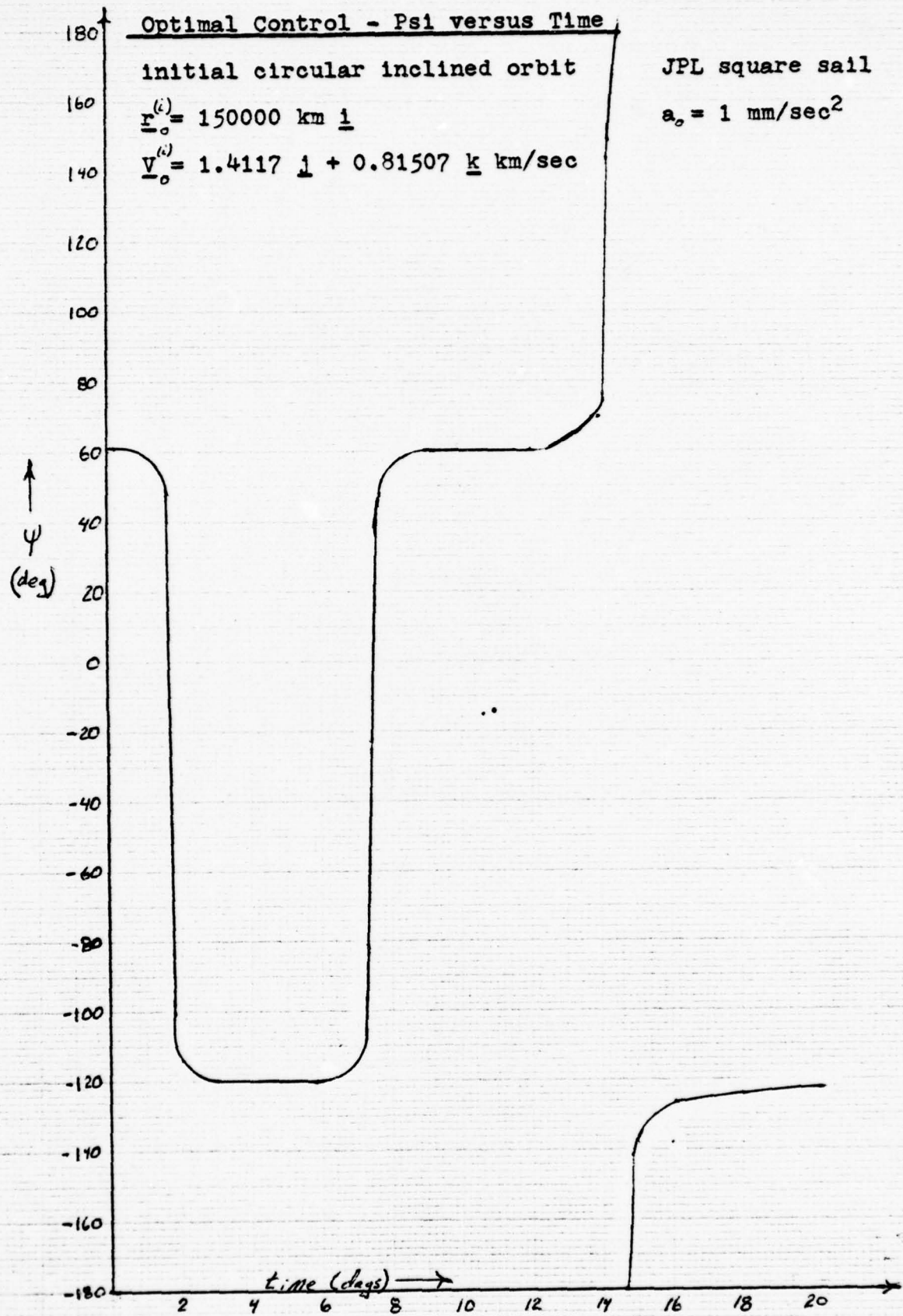


Figure 12

Optimal Control - Theta versus Time

initial circular polar orbit $r^{(0)} = 150000 \text{ km}$ k
JPL square sail $a_s = 1 \text{ mm/sec}^2$ $v^{(0)} = 1.63014 \text{ km/sec}$ l



Figure 13

Optimal Control - Psi versus Time

initial circular polar orbit - $r_0^{(i)} = 150000 \text{ km}$ k

JPL square sail

$v_0^{(i)} = 1.63014 \text{ km/sec}$ l

$a_0 = 1 \text{ mm/sec}^2$

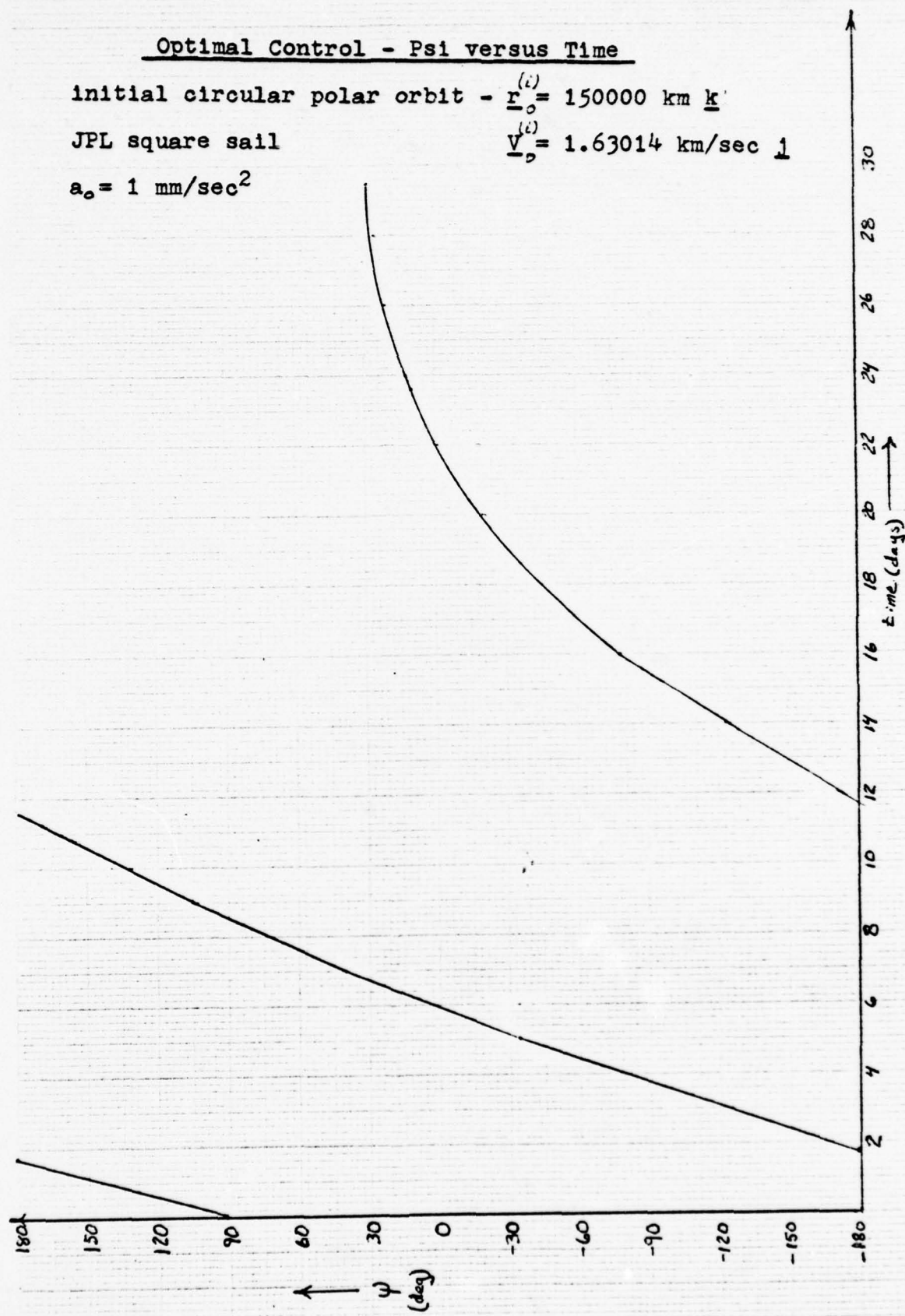


Figure 14

Optimal Control - Eccentricity versus Time

initial circular polar orbit - $r_o^{(i)} = 15000$ km k

$v_o^{(i)} = -1.63014$ km/sec l

JPL square sail - $a_o = 1$ mm/sec 2

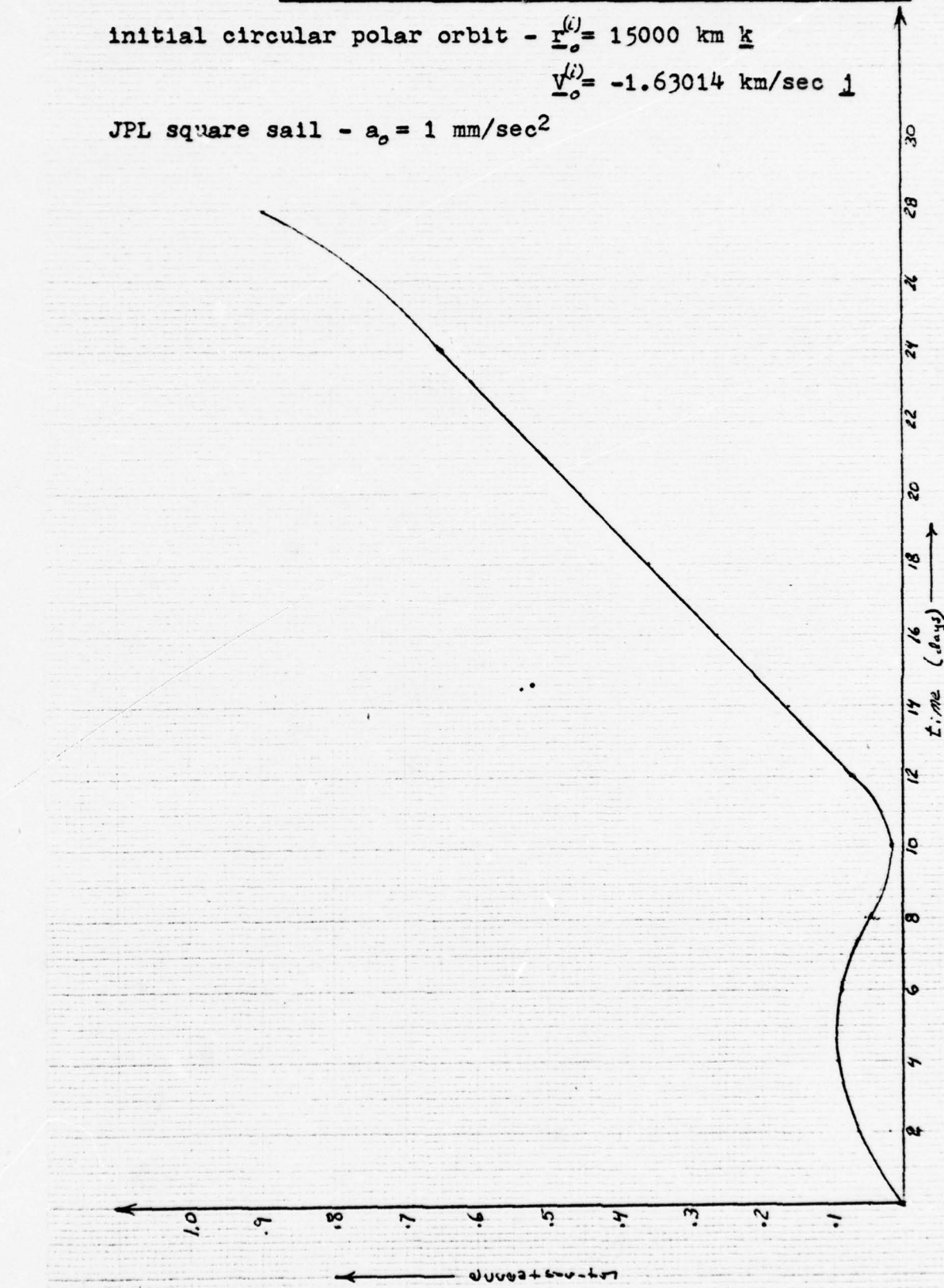
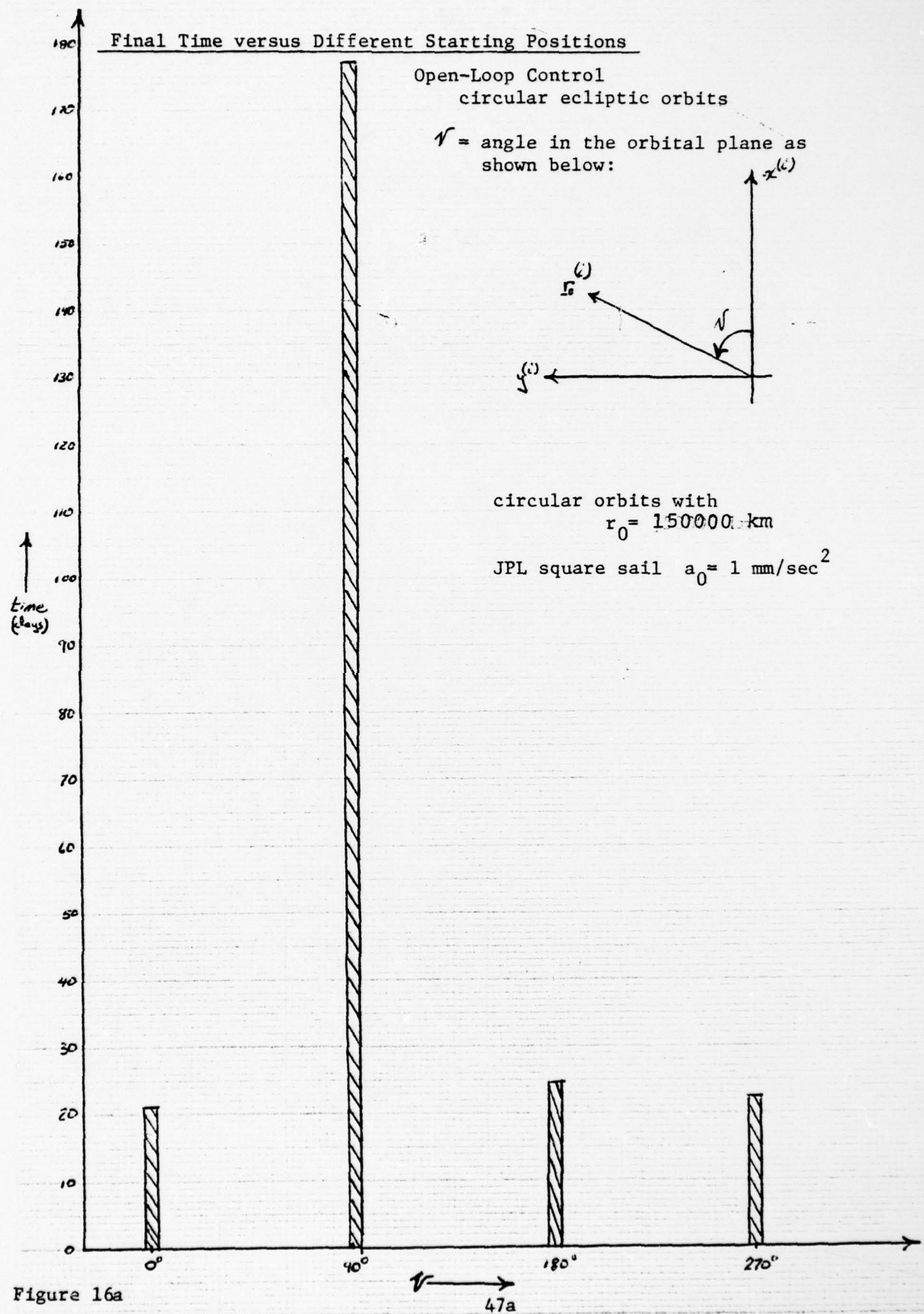
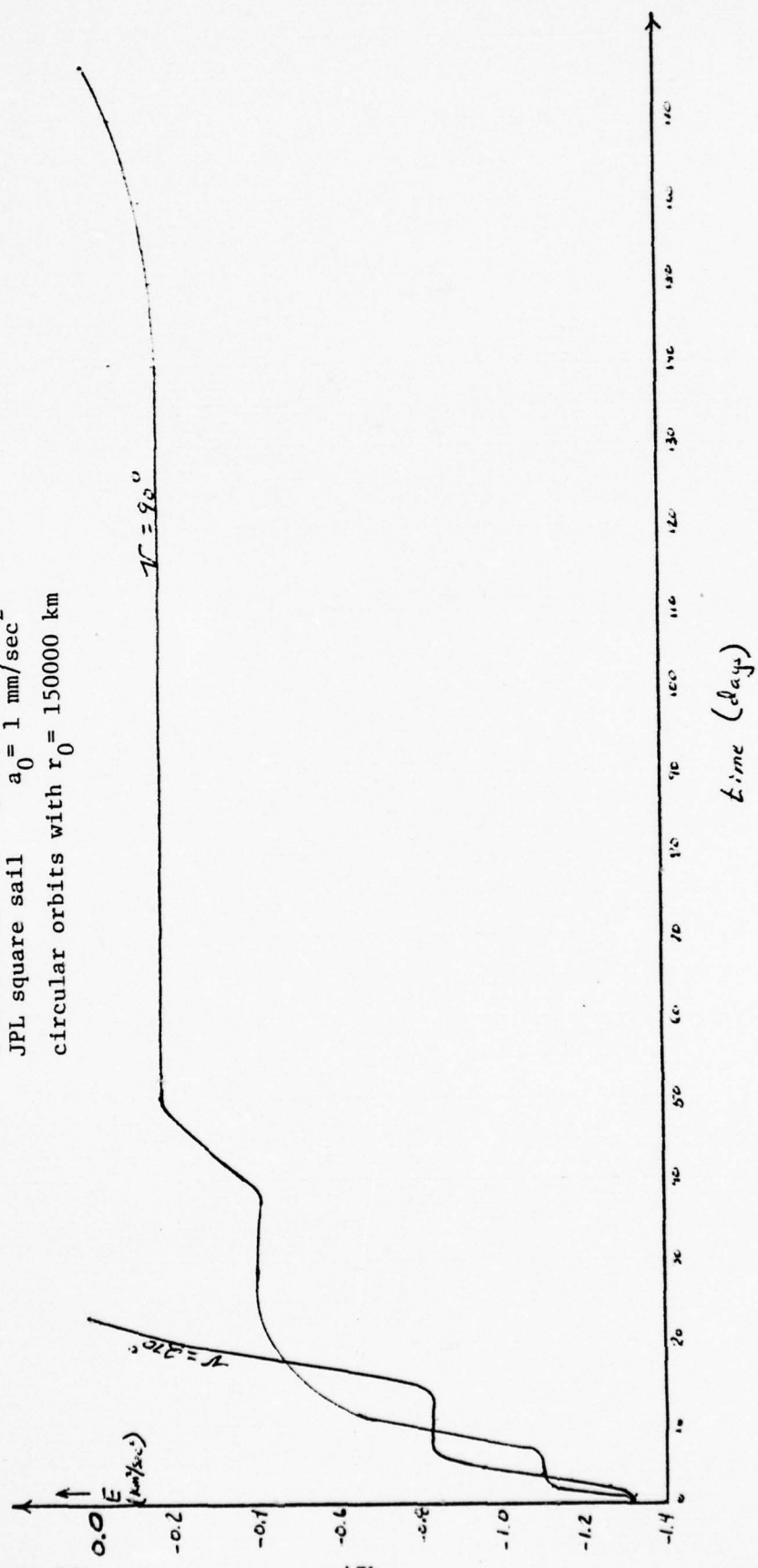


Figure 15



Energy versus Time for Different Starting Positions

open-loop control.
 ν as defined in figure 16a
JPL square sail $a_0 = 1 \text{ mm/sec}^2$
circular orbits with $r_0 = 150000 \text{ km}$



Final Time versus Different Starting Positions

velocity-dependent control JPL square sail $a_0 = 1 \text{ mm/sec}^2$

circular polar orbits with $r_0 = 150000 \text{ km}$

ν = angle in the orbital plane
as shown below:

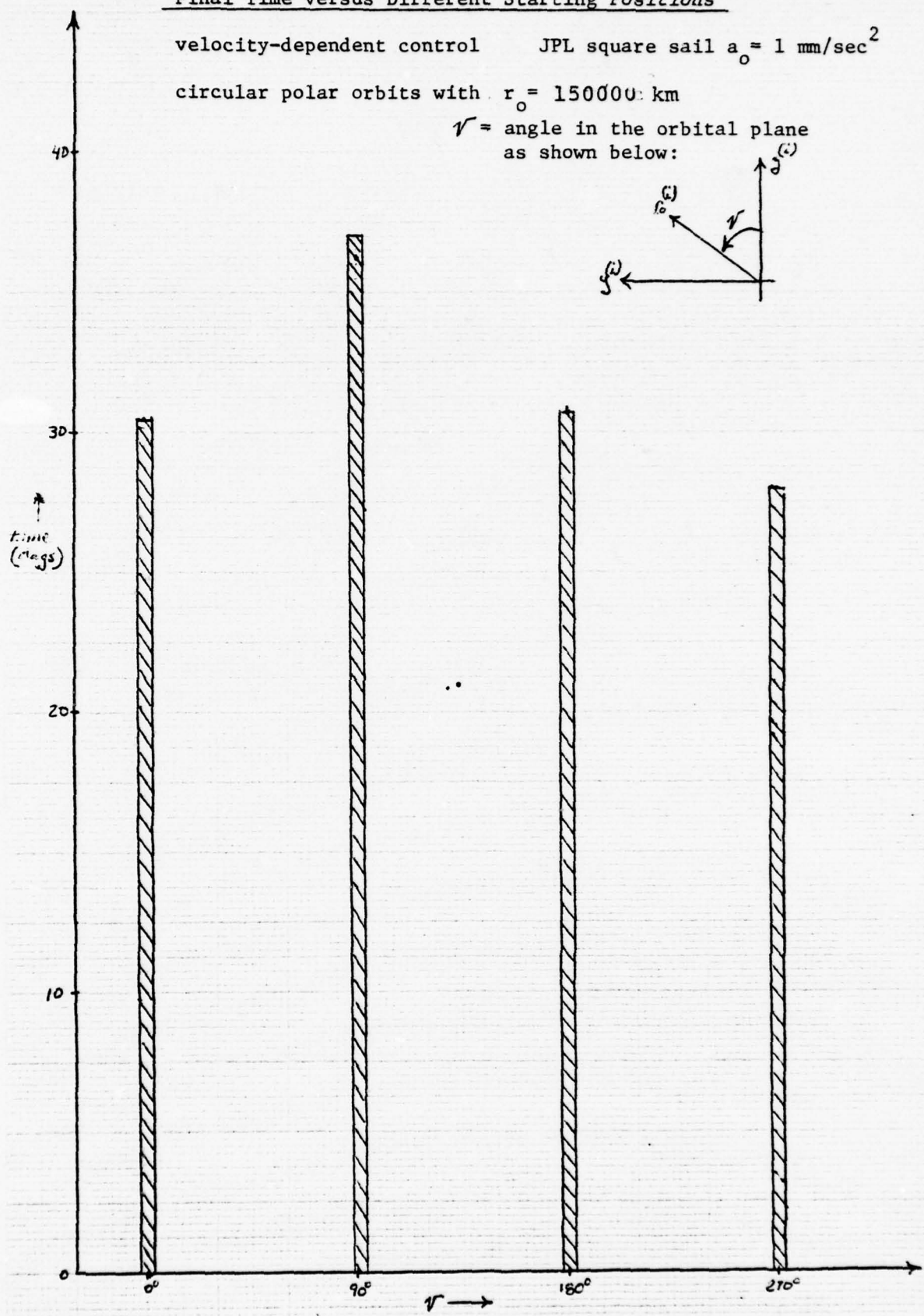
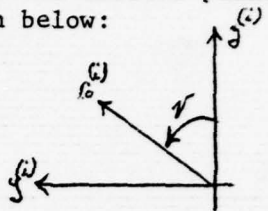


Figure 17a

48a

Energy versus Time for $\gamma = 0^\circ$

velocity-dependent control JPL square sail $a_0 = 1 \text{ mm/sec}^2$
circular polar orbits with $r_0 = 150000 \text{ km}$
 γ as defined in figure 17a

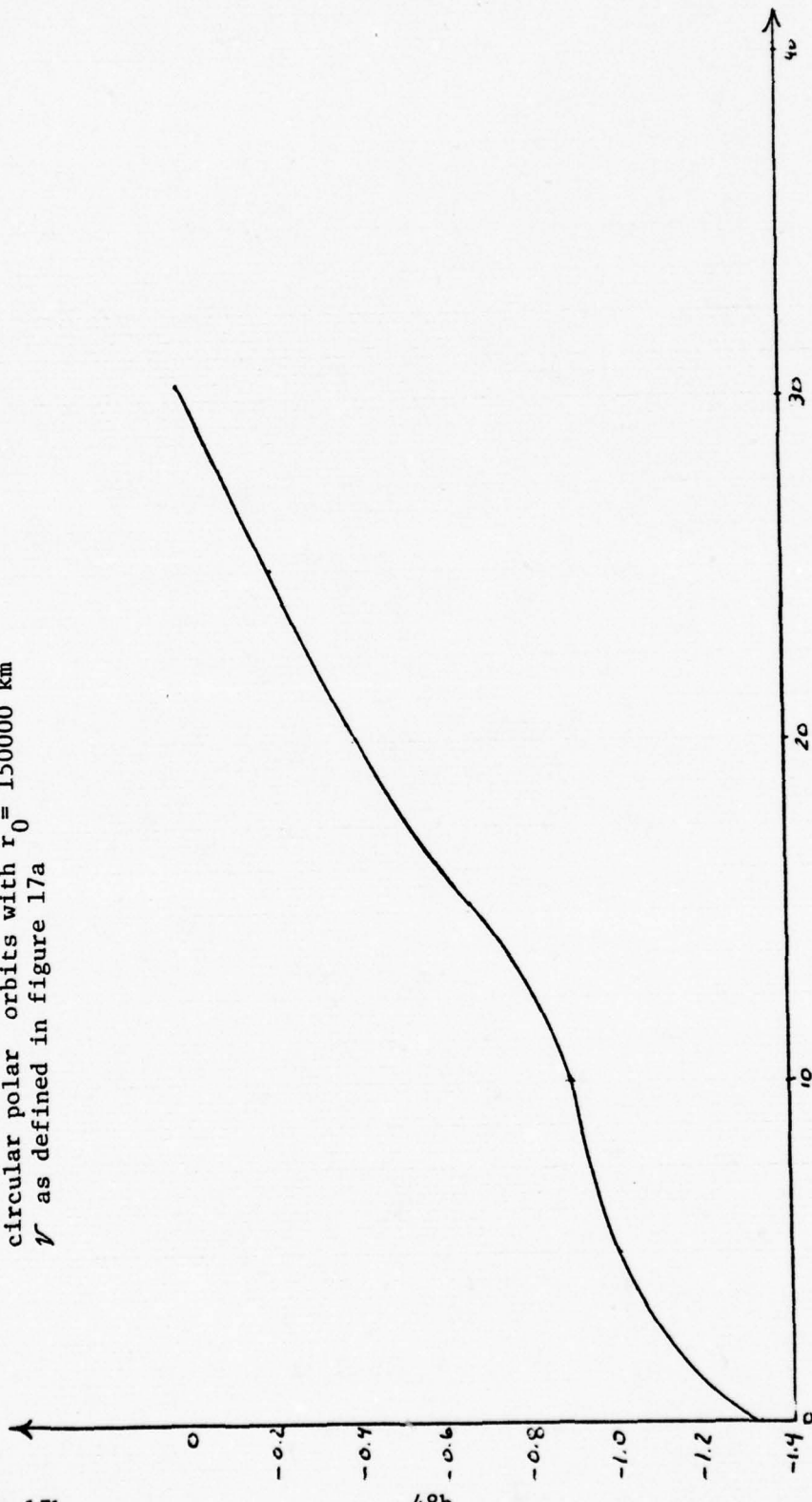


Figure 17b

CONCLUSIONS

1. Escape from a high Earth orbit with solar sail propulsion is possible.
2. Optimal escape trajectories in the ecliptic plane will give the minimum escape time, but will demand the greatest attitude rates. Ecliptic escape trajectories involve very fast increases in eccentricity, with semi-major axes perpendicular to the Sun-spacecraft line. Escape time from ecliptic orbits is dependent upon the initial energy of the spacecraft, the starting position of the vehicle in the orbit, and the eccentricity of the initial orbit.
3. Optimal polar escape trajectories will have the least demanding attitude rates, but the escape times will be longer than similar inclined and ecliptic escape trajectories. Polar escape trajectories maintain a low eccentricity throughout most of the trajectory. Escape time from polar orbits is dependent upon the initial energy of the spacecraft. Starting position in the orbit and the eccentricity of the initial orbit have little effect upon the final escape time for polar escape trajectories.
4. The performance of optimal escape trajectories inclined with respect to the ecliptic plane will tend to be between the limiting cases of similar polar and ecliptic escape trajectories.

5. Open-loop control is a good approximation to the optimal control law of a minimum time escape with a solar sail from a high Earth orbit with low inclination and low eccentricity.
6. Open-loop control, with the proper scale factor, serves as a good initial guess for the co-state vectors in the determination of the optimal control law. The scale factor should be chosen such that the final co-state is of the same order of magnitude as the calculated optimal final co-state (equation 32).
7. Velocity-dependent control serves as a good approximation for the optimal control law of a minimum time escape from a high Earth orbit.

BIBLIOGRAPHY

1. Battin, R.H. Astronautical Guidance. New York, New York: McGraw-Hill, 1964.
2. Bryson, A.E., Jr. and Yu-Chi Ho. Applied Optimal Control. Waltham, Massachusetts: Ginn and Company, 1969.
3. Cunningham, J.D. Optimal Control of a Solar Radiation Pressure Powered Space Vehicle. (ad/a-004-792) Unpublished MS thesis. Wright-Patterson Air Force Base, Ohio: Air Force Institute of Technology, December, 1974.
4. Fimple, W.R. "A Generalized 3 Dimensional Trajectory Analysis of Planetary Escape by Solar Sail," ARS Journal, 32:883-887 (June, 1962).
5. Grodzovshii, G.L., Yu.N. Ivanov and V.V. Tokarev. Mechanics of Low Thrust Spaceflight. Translated from Russian by A. Baruch. Jerusalem, Israel: IPST Press, 1969.
6. Hyde, Roderick A. Design and Behavior of Ribless Solar Reflectors. Unpublished Ph.D thesis. Cambridge, Massachusetts: Massachusetts Institute of Technology, 1976.
7. London, H.S. "Some Exact Solutions to the Equations of Motion of a Solar Sail with Constant Sail Settings," ARS Journal, 30:198-200 (February, 1960).

8. Sacket,L.L and T.N. Edelbaum. "Optimal Solar Sail Spiral to Escape," to be presented at the AIAA/AAS Astrodynamics Conference, September, 1977.
9. Sacket,L.L.,H.L.Malchow and T.N.Edelbaum. Solar Electric Geocentric Transfer with Attitude Constraints: Analysis. NASA CR-134927(Draper Lab R-901), Cambridge, Massachusetts: The Charles Stark Draper Laboratory, Inc., August, 1975.
10. Sacket,L.L., H.L. Malchow and T.N. Edelbaum. Solar Electric Geocentric Transfer with Attitude Constraints: Program Manual. Report R-902, Cambridge, Massachusetts: The Charles Stark Draper Laboratory, Inc., August,1975.
11. Sands,N. "Escape from Planetary Gravitational Fields by use of Solar Sails," ARS Journal, 31:527-531(April,1961).
12. Sauer,C.G.,Jr."Optimum Solar-Sail Interplanetary Trajectories," Paper 76-792, AIAA/AAS Astrodynamics Conference, San Diego, California, August,1976.
13. Schultz,D.G. and J.L. Melsa. State Functions and Linear Control Systems. New York, New York: McGraw-Hill,1967.
14. Tsu,T.C. "Interplanetary Travel by Solar Sail," ARS Journal, 29:422-427(June,1959).

15. Villers, P. On the Application of Solar Radiation Momentum Transfer to Space Vehicle Propulsion. Unpublished MS thesis. Cambridge, Massachusetts: Massachusetts Institute of Technology, 1960.
16. Wright, J.L. "Solar Sail Force Model," Jet Propulsion Laboratory Interoffice Memorandum (312/77.3-201). 28 March 1977.
17. Wright, J.L. and J. Warmke, "Solar Sail Mission Applications," Paper 76-808, AIAA/AAS Astrodynamics Conference, San Diego, California, August, 1976.

APPENDIX A
Force Equation Parameters

The values of all constants used in this thesis are:

	<u>Perfect Sail</u>	<u>JPL Square Sail</u>	<u>JPL Heliogyro Sail</u>
r	1	0.88	0.88
s	1	0.94	0.94
ϵ_r	0	0.05	0.05
ϵ_b	0	0.55	0.55
B_r	2/3	0.79	0.79
B_b	2/3	0.55	0.55
c_1	0.5	0.349	0.367
c_2	0.5	0.662	0.643
c_3	0	-0.011	-0.010

The values for the constants in the JPL square and heliogyro sails were obtained from a JPL interoffice memorandum dated 28 March 1977 (ref 16). These are the proposed specifications on possible future solar sails being considered by the Jet Propulsion Laboratory. At high altitudes, where the attitude controls are slowly varying, the heliogyro sail can be approximated by the model developed in this thesis.

Typical values of a_o for the JPL square and heliogyro sails vary from about 0.3 to 1.2 millimeters/sec². This thesis assumes an a_o of 1 mm/sec² for all calculations.

Figure A-1 is a graph of the normalized force versus θ for the three types of solar sails listed above. Equation 8 is the generating function. The quantity θ is the cone angle of the sail's force vector with respect to the x axis of the rotating coordinate frame (see figure 5).

Figures A-2 and A-3 are polar plots of equation 11 for the ideal and JPL square sail. The polar plots are in the plane of the primer vector and the Sun-spacecraft line. The only quadrant of concern is the upper right quadrant since this is where θ satisfies equation 17. The upper constraint on the cone angle in equation 17 (180 degrees) results from the mathematical definition of a cone angle. The lower constraint in equation 17 (θ_L) results from the physical fact that the sail's force vector can never point toward the Sun. From figure A-1 it can be seen that θ_L is around 118 degrees. Figures A-2 and A-3 also show the basic principle behind the optimal θ . Given the direction of a primer vector, the optimal θ is the angle that maximizes the projection of \underline{F} onto λ_p . When β is less than β_L , the maximum projection of \underline{F} onto λ_p results when \underline{F} equals zero or θ equals θ_L .

Figure A-4 is a plot of the centerline angle (ϕ) versus the cone angle (θ). The centerline angle is the angle between the sail's normal and the thrust vector (see figure 4). The analysis developed in this thesis determines the optimal θ . Using figure A-4 or an analytical representation, the corresponding optimal ϕ can be determined. The following equation can be used to find the incident angle α (see figure 4):

$$\alpha = 180^\circ - \theta + \phi \quad (A-1)$$

The analysis developed in this thesis also determines the optimal ψ of the force vector (see figure 5). Knowing ψ and α , the orientation of the solar sail is defined and the sail can then be positioned in space to achieve the optimal thrust.

Normalized Force versus Theta

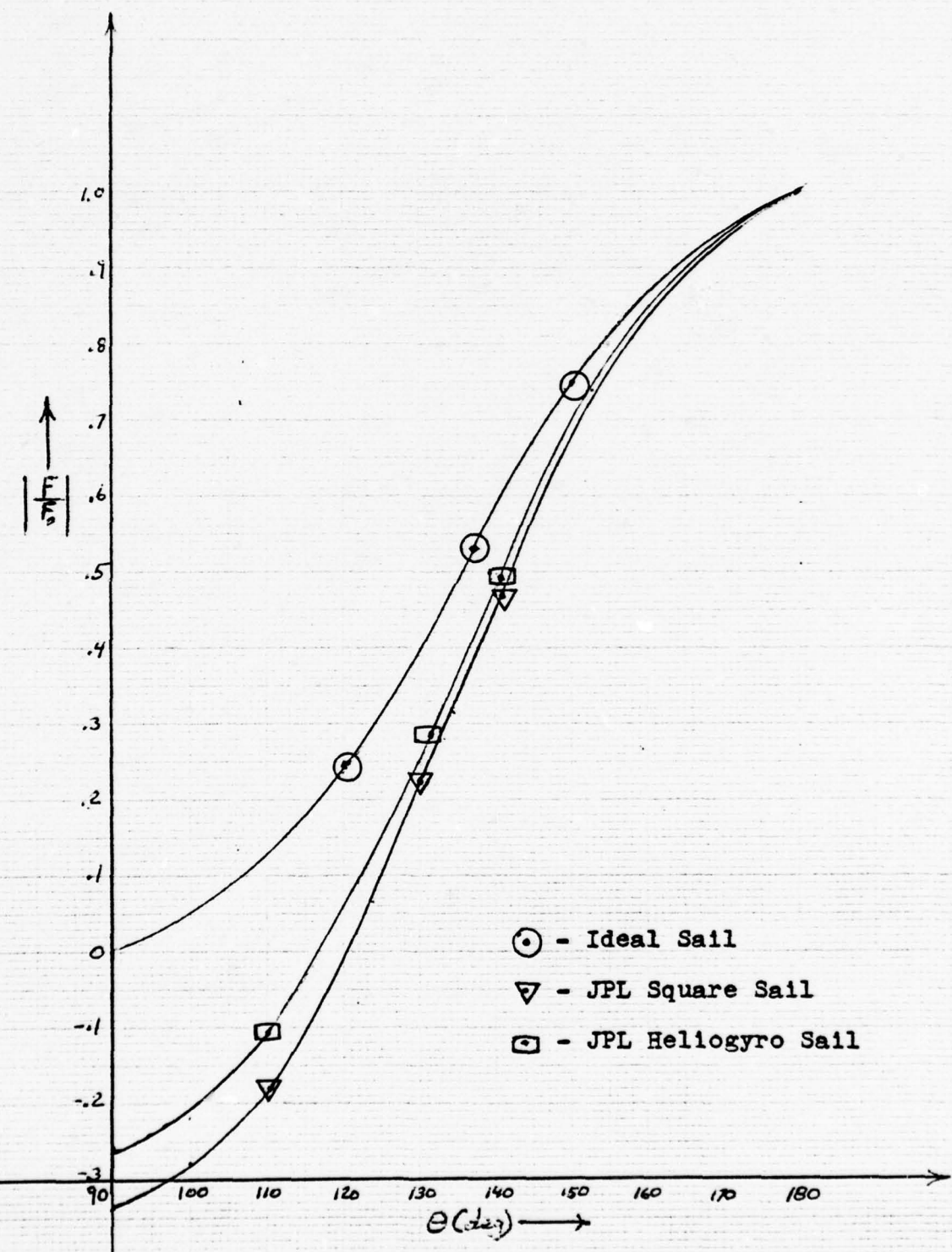


Figure A-1

Polar Plot of Normalized Acceleration Vector for Ideal Sail

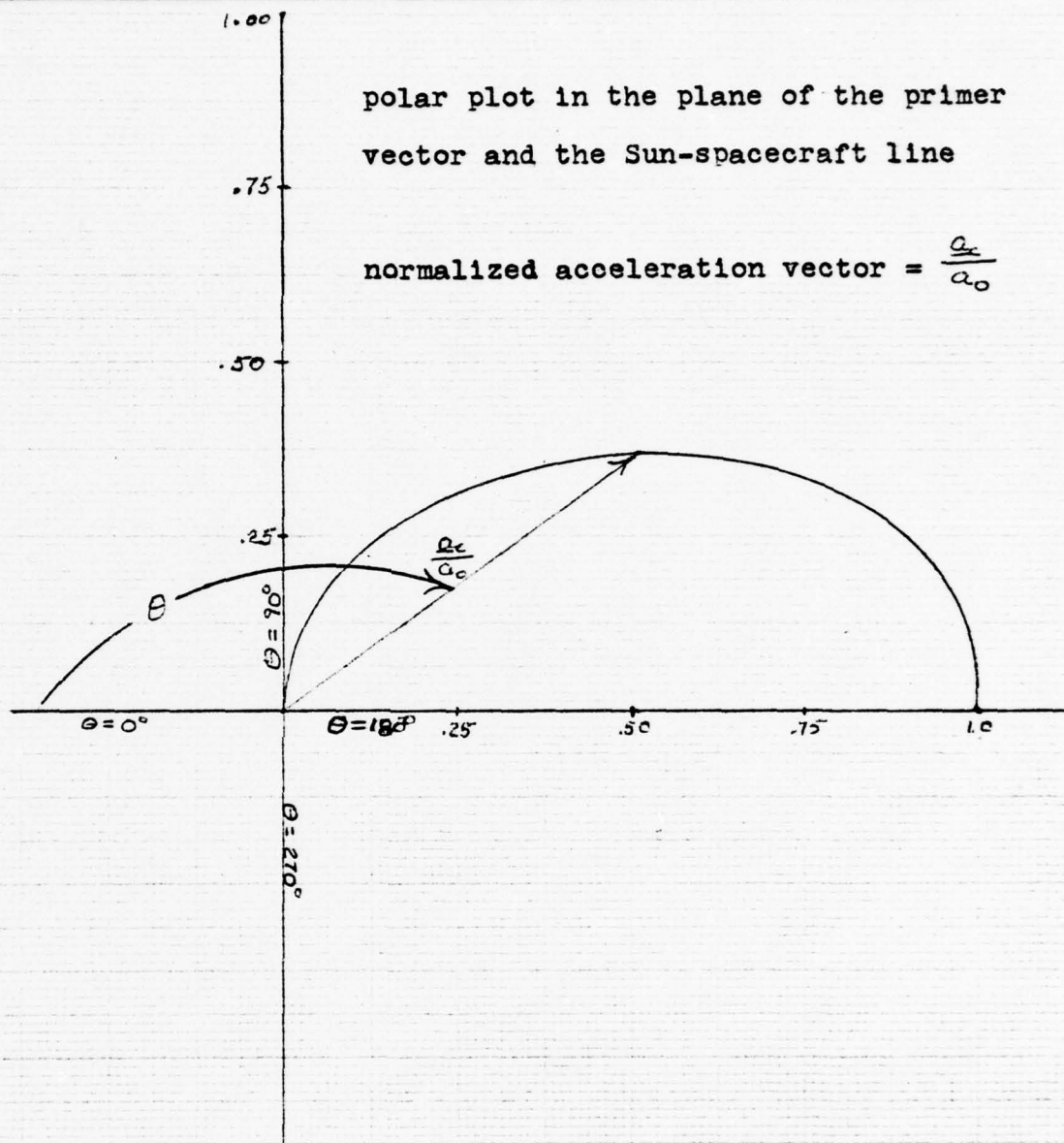
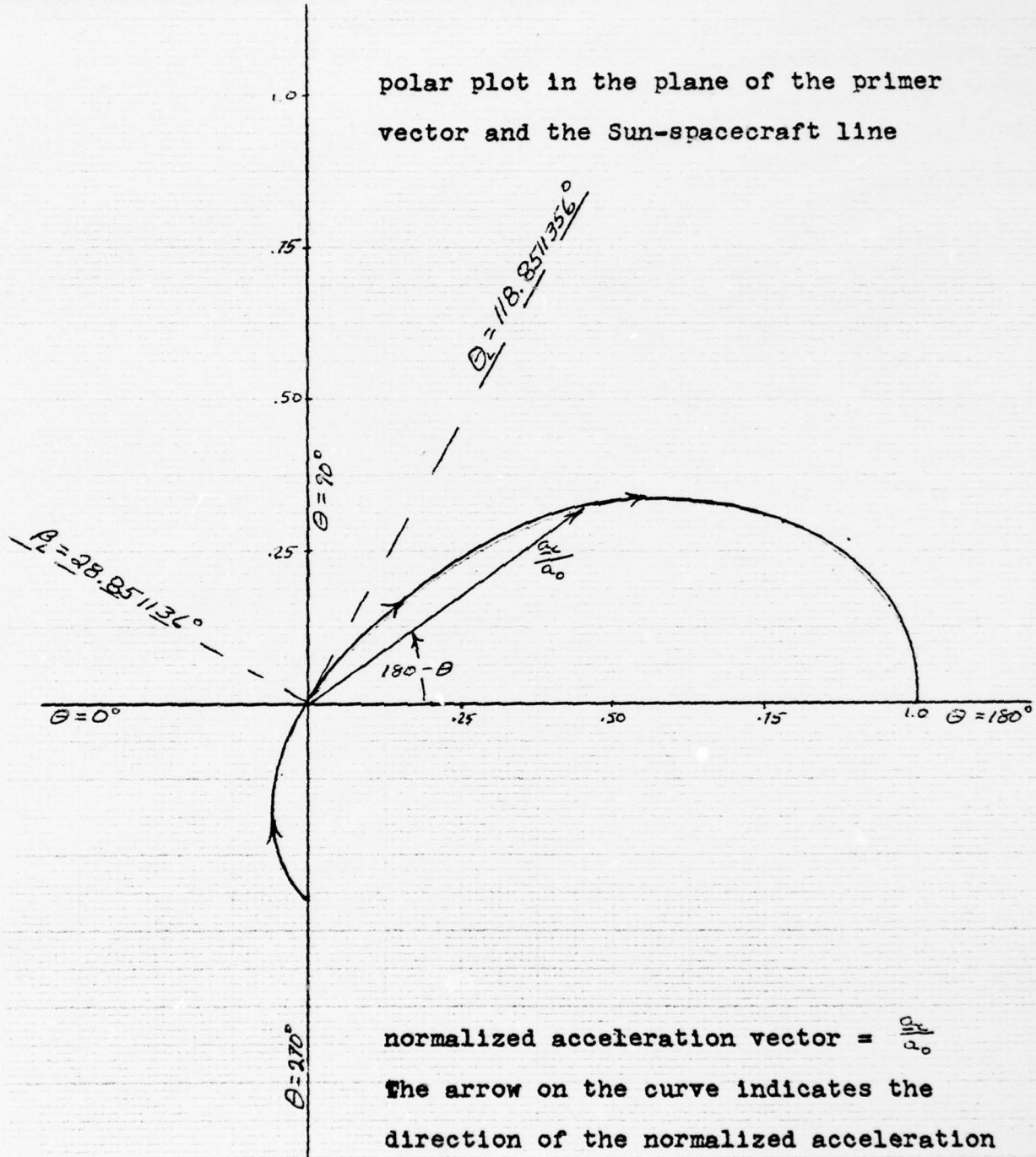


Figure A-2

Polar Plot of Normalized Acceleration Vector for JPL Square Sail



normalized acceleration vector = $\frac{\alpha_x}{\alpha_0}$
The arrow on the curve indicates the direction of the normalized acceleration vector as theta goes from 90 degrees to 180 degrees. When theta is less than θ_c the acceleration vector is negative.

Figure A-3

Centerline Angle versus Cone Angle

JPL square sail with $c_s = 0.35$

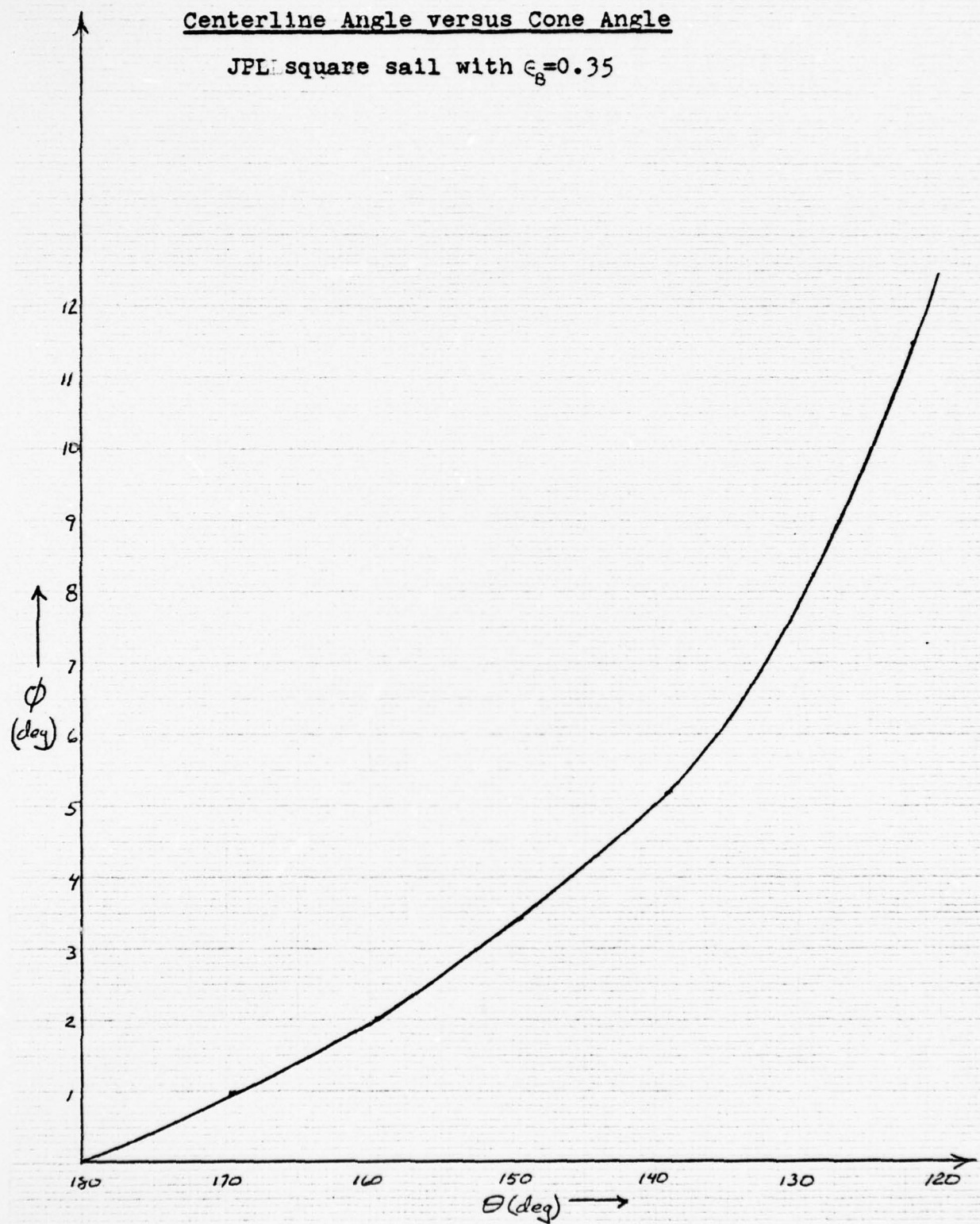


Figure A-4

APPENDIX B
Optimal Control Theory

This appendix develops the basic theory of optimal control used in this thesis (ref 2 and 13).

Let the integral I be defined as:

$$I = \int_{t_i}^{t_f} F(\underline{x}, \dot{\underline{x}}, t) dt \quad (B-1)$$

If the problem is to find the function \underline{x} that maximizes I , the integrand must satisfy the Euler-Lagrange equation (ref 13):

$$\frac{\partial F}{\partial \underline{x}} - \frac{d}{dt} \left[\frac{\partial F}{\partial \dot{\underline{x}}} \right] = 0 \quad (B-2)$$

Also if the end point \underline{x}_1 is assumed to be fixed (\underline{x}_1 and t_1 specified), the following generalized boundary condition must be satisfied (ref 13):

$$\left[\left[\frac{\partial F}{\partial \dot{\underline{x}}} \right] S \underline{x} + \left[F - \left(\frac{\partial F}{\partial \dot{\underline{x}}} \right) \dot{\underline{x}} \right] S t \right]_{t=t_f} = 0 \quad (B-3)$$

The problem that this thesis is concerned with is the minimization of the performance index J :

$$J = S + \int_{t_i}^{t_f} L dt \quad (B-4)$$

where

$S = S(\underline{x}(t_f), t_f)$

$L = L(\underline{x}, \underline{u}, t)$

\underline{x} = state

\underline{u} = control

t_f = final time (free)

t_i = initial time (fixed)

It is also assumed that the following constraint equations are imposed:

$$\dot{\underline{x}} = \underline{f}(\underline{x}, \underline{u}, t) \quad (\text{state equations})$$

$$\underline{\Psi}(\underline{x}(t_f), t_f) = 0 \quad (\text{functions specified at final time})$$

Using the method of Lagrange multipliers, the constraint equations can be adjoined to J , and therefore the redefined performance index J' can be treated in an unconstrained problem. Therefore:

$$J' = S'(\underline{x}(t_f), t_f) + \int_{t_i}^{t_f} [L + \dot{\underline{\lambda}}^T(\dot{\underline{x}} - \underline{f})] dt$$

where

$$S'(\underline{x}(t_f), t_f) = S + \underline{\nu}^T \underline{\Psi}$$

$\underline{\nu}$ - Lagrange multiplier for constraint at final time.

$\dot{\underline{\lambda}}$ - Lagrange multiplier for state equations (co-state).

The following performance index can be defined:

$$PI = \int_{t_i}^{t_f} [L + \dot{\underline{\lambda}}^T(\dot{\underline{x}} - \underline{f})] dt + S'(\underline{x}(t_f), t_f) - S'(\underline{x}(t_i), t_i)$$

Since $\underline{x}(t_1)$ and t_1 are assumed fixed the minimization of PI is the same as the minimization of J' . Therefore J' can be re-written as:

$$J' = \int_{t_1}^{t_f} \left[L + \underline{\lambda}^T (\dot{\underline{x}} - \underline{f}) + \frac{ds'}{dt} \right] dt$$

By use of the chain rule this can be re-written as:

$$J' = \int_{t_1}^{t_f} \left[L + \left(\frac{\partial S'}{\partial \underline{x}} \right) \dot{\underline{x}} + \frac{\partial S'}{\partial t} - \underline{\lambda}^T \underline{f} + \underline{\lambda}^T \dot{\underline{x}} \right] dt$$

Defining the Hamiltonian H such that maximizing it minimizes J :

$$H(\underline{x}, \underline{u}, \underline{\lambda}, t) = -L + \underline{\lambda}^T \underline{f} \quad (B-5)$$

Therefore J' can be re-written as

$$J' = \int_{t_1}^{t_f} \left[\left(\frac{\partial S'}{\partial \underline{x}} \right) \dot{\underline{x}} + \frac{\partial S'}{\partial t} - H + \underline{\lambda}^T \dot{\underline{x}} \right] dt = \int_{t_1}^{t_f} L'(\dot{\underline{x}}, \underline{x}, \underline{u}, \underline{\lambda}, t) dt \quad (B-6)$$

Applying the Euler-Lagrange equation to J' and remembering that \underline{x} in equation B-2 corresponds to \underline{x} and \underline{u} in equation B-6

$$\frac{\partial L'}{\partial \underline{x}} - \frac{d}{dt} \left[\frac{\partial L'}{\partial \dot{\underline{x}}} \right] = 0$$

$$- \frac{\partial H}{\partial \underline{x}} - \frac{d}{dt} \left[\frac{\partial S'}{\partial \underline{x}} + \underline{\lambda}^T \right] = 0$$

$$\dot{\underline{\lambda}} = - \left[\frac{\partial H}{\partial \underline{x}} \right]^T \quad (B-7)$$

$$\frac{\partial L'}{\partial \underline{u}} - \frac{d}{dt} \left[\frac{\partial L'}{\partial \dot{\underline{u}}} \right] = 0$$

$$\frac{\partial H}{\partial u} = 0 \quad (B-8)$$

Also, from inspection of the Hamiltonian, the following expression can be obtained:

$$\left[\frac{\partial H}{\partial \dot{x}} \right]^T = \dot{x} \quad (B-9)$$

Applying the generalized boundary condition (equation B-3), the following expression can be written:

$$\left\{ \left[\frac{\partial L'}{\partial \dot{x}} \right] S_x + \left[L' - \left(\frac{\partial L'}{\partial \dot{x}} \right) \dot{x} \right] S_t \right\}_{t=t_f} = 0$$

Substitution of L' gives the following:

$$\left\{ \left[\frac{\partial S'}{\partial \dot{x}} + \lambda^T \right] S_x + \left[\left(\frac{\partial S'}{\partial \dot{x}} \right) \dot{x} + \frac{\partial S'}{\partial t} - H + \lambda^T \dot{x} - \left(\frac{\partial S'}{\partial \dot{x}} + \lambda^T \right) \dot{x} \right] S_t \right\}_{t=t_f} = 0$$

Substitution of S' and H and rearranging terms gives:

$$\left\{ \left[\frac{\partial S}{\partial \dot{x}} + \lambda^T \frac{\partial \Psi}{\partial \dot{x}} + \lambda^T \right] S_x + \left[L - \lambda^T f + \frac{\partial S}{\partial t} + \lambda^T \frac{\partial \Psi}{\partial t} \right] S_t \right\}_{t=t_f} = 0$$

therefore

$$\lambda_f = - \left[\frac{\partial S}{\partial \dot{x}} + \lambda^T \frac{\partial \Psi}{\partial \dot{x}} \right]_{t=t_f}^T \quad (B-10a)$$

$$\left[\frac{\partial S}{\partial t} + \lambda^T \frac{\partial \Psi}{\partial t} + L + \left(\frac{\partial S}{\partial \dot{x}} + \lambda^T \frac{\partial \Psi}{\partial \dot{x}} \right) f \right]_{t=t_f} = 0 \quad (B-10b)$$

$$\Psi(x(t_f), t_f) = \underline{\underline{\Omega}} \quad (B-10c)$$

Therefore in order to minimize equation B-4, a Hamiltonian, defined as in equation B-5, must be maximized. Equations B-7, B-8 and B-9 give the differential equations and control law that must be satisfied, subject to the boundary conditions on the state at the initial time and the co-state at the final time (equation B-10), in order to determine the optimal escape trajectory.

APPENDIX C

An Energy Dependent Newton-Raphson Iterator

The solution to the problem of minimizing the final time on an Earth escape maneuver to zero energy has been shown to be the solution of the following set of coupled differential equations:

$$\dot{\underline{r}}^{(i)} = \underline{v}^{(i)} \quad (C-1a)$$

$$\dot{\underline{v}}^{(i)} = \underline{\alpha}_c^{(i)} - \frac{\mu \underline{r}^{(i)}}{r^3} \quad (C-1b)$$

$$\dot{\underline{\lambda}}_r^{(i)} = \frac{\mu}{r^3} \underline{\lambda}_v^{(i)} - \frac{3\mu}{r^5} \left(\underline{\lambda}_v^{(i)T} \cdot \underline{r}^{(i)} \right) \underline{r}^{(i)} \quad (C-1c)$$

$$\dot{\underline{\lambda}}_v^{(i)} = -\underline{\lambda}_r^{(i)} \quad (C-1d)$$

The optimal control variables, θ and ψ , are determined by equations 24 and 27 in conjunction with equation 28 and 29. The boundary conditions for the above set of differential equations are:

$$\underline{r}^{(i)}(0) = \underline{r}_0 \quad (C-2a)$$

$$\underline{v}^{(i)}(0) = \underline{v}_0 \quad (C-2b)$$

$$\underline{\lambda}_r^{(i)}(t_f) = \left[\frac{\mu \underline{r}^{(i)}}{r^3 (\underline{v}^{(i)T} \cdot \underline{\alpha}_c^{(i)})} \right]_{t=t_f} \quad (C-2c)$$

$$\underline{\lambda}_r^{(i)}(t_f) = \left[\frac{\underline{v}^{(i)}}{(\underline{v}^{(i)T} \cdot \underline{\lambda}_c^{(i)})} \right]_{t=t_f} \quad (C-2d)$$

$$E[\underline{\lambda}(t_f)] = E_f \quad (C-2e)$$

where

$$E[\underline{\lambda}(t)] = \frac{\underline{v}^{(i)T} \cdot \underline{v}^{(i)}}{2} - \frac{\mu}{(\underline{r}^{(i)T} \cdot \underline{r}^{(i)})^{\frac{1}{2}}} \quad (C-3)$$

and * denotes the optimal end conditions as developed in Appendix B. For an escape trajectory E_f is zero.

As can be seen, this is a two-point boundary value problem. The method of solution will be to guess $\underline{\lambda}_r^{(0)}$ and $\underline{\lambda}_v^{(0)}$ and then integrate equation C-1 forward until equation C-2e is satisfied. The results of equations C-2c and C-2d are then compared to the final co-state of the numerical integration. If the two co-states agree to within a desired accuracy, the problem is solved. If they do not agree, an iteration scheme will be used to improve the initial guess on the co-state. This iteration scheme is developed as follows.

Define the following function h :

$$h = \underline{\lambda}^{(i)}(t_f) - \underline{\lambda}^{(i)*}(t_f) \quad (C-4)$$

where

$$\underline{\lambda}^{(i)}(t_f) = \left[\underline{\lambda}_r^{(i)}, \underline{\lambda}_v^{(i)} \right]^T_{t=t_f} \quad (\text{from numerical integration})$$

$$\underline{\lambda}^{(i)*}(t_f) = \left[\underline{\lambda}_r^{(i)*}, \underline{\lambda}_v^{(i)*} \right]^T_{t=t_f} \quad (\text{from equation C-2c and C-2d})$$

If it is assumed that as $E(\underline{x}(t))$ approaches E_f , energy is a monotonic increasing function, a one-to-one mapping will exist between t_f and E_f . In other words if a given E_f is specified for a given initial state and co-state, the final time is uniquely specified. If E_f is changed, t_f changes correspondingly. It is also evident that if E_f is held fixed and the initial co-state is varied, $t_f, \underline{x}(t_f), \lambda(t_f)$ and \underline{h} will all vary. The quantity \underline{h} is therefore a function of the initial co-state and the specified terminating energy condition for a fixed initial state. This can be represented as:

$$\underline{h} = \underline{h}(\lambda^{(i)}(0), E_f) \quad (c-5)$$

By use of a Taylor's series expansion, the following is true to first order:

$$\underline{h}(\lambda^{(i)}(0) + \delta \lambda^{(i)}(0), E_f + \delta E_f) = \underline{h}(\lambda^{(i)}(0), E_f) + \left[\frac{\partial \underline{h}}{\partial \lambda^{(i)}(0)} \right]_{E_f} \delta \lambda^{(i)}(0) + \left[\frac{\partial \underline{h}}{\partial E_f} \right]_{\lambda^{(i)}(0)} \delta E_f + \dots$$

For the problem defined in this thesis, E_f is fixed; therefore δE_f equals zero. Also the desired change in $\lambda(0)$ should be such that to first order, \underline{h} is driven to zero (final co-state and optimal final co-state are equal). Therefore:

$$\underline{\Omega} = \underline{h}(\lambda^{(i)}(0), E_f) + \left[\frac{\partial \underline{h}}{\partial \lambda^{(i)}(0)} \right]_{E_f} \delta \lambda^{(i)}(0)$$

Define the matrix G as follows:

$$G = \left[\frac{\partial \underline{h}}{\partial \lambda^{(i)}(0)} \right]_{E_f}$$

Rearranging terms and substitution gives:

$$\int \underline{\lambda}^{(i)}(0) = - G^{-1} \left[\underline{\lambda}^{(i)}(t_f) - \underline{\lambda}^{(i)*}(t_f) \right]_{E=E_f} \quad (C-6)$$

The improved guess on the initial co-state can be written as:

$$\left[\underline{\lambda}^{(i)}(0) \right]_{\text{new}} = \left[\underline{\lambda}^{(i)}(0) \right]_{\text{old}} + \int \underline{\lambda}^{(i)}(0) \quad (C-7)$$

The implementation of equation C-6 requires the determination of the matrix G. Analytically this is very difficult. The method used in this thesis is to calculate neighboring trajectories. The development of equation C-5 has shown that this problem can be considered in an "energy space" instead of the conventional "time space". Each neighboring trajectory should therefore be terminated when the energy equals E_f . The result of this technique is that G is a six-by-six matrix and six neighboring trajectories need to be calculated on each iteration.

An obvious difficulty of working in a so-called "energy space" is that equation C-1 has to be integrated in a "time space". Since the Runge-Kutta integration scheme takes finite time steps, satisfaction of the energy stopping condition will generally occur between integration steps. A simple interpolation is used to adjust the size of the last integration step. This is shown graphically in figure C-1.

When the energy becomes greater than E_f on a particular step, the average slope of the energy curve over the last step

is determined as

$$m = \frac{E_n - E_0}{t_n - t_0} \quad (C-8)$$

The stepsize ss_n , which, if taken from t_0 , will yield an energy approximately equal to E_f at $t=t_0+ss_n$, can be expressed as:

$$ss_n = \frac{-E_0}{m} \quad (C-9)$$

The state and co-state are re-initialized to their values at $t=t_0$, and the time step ss_n is taken so that condition $E=E_f$ is approximately achieved.

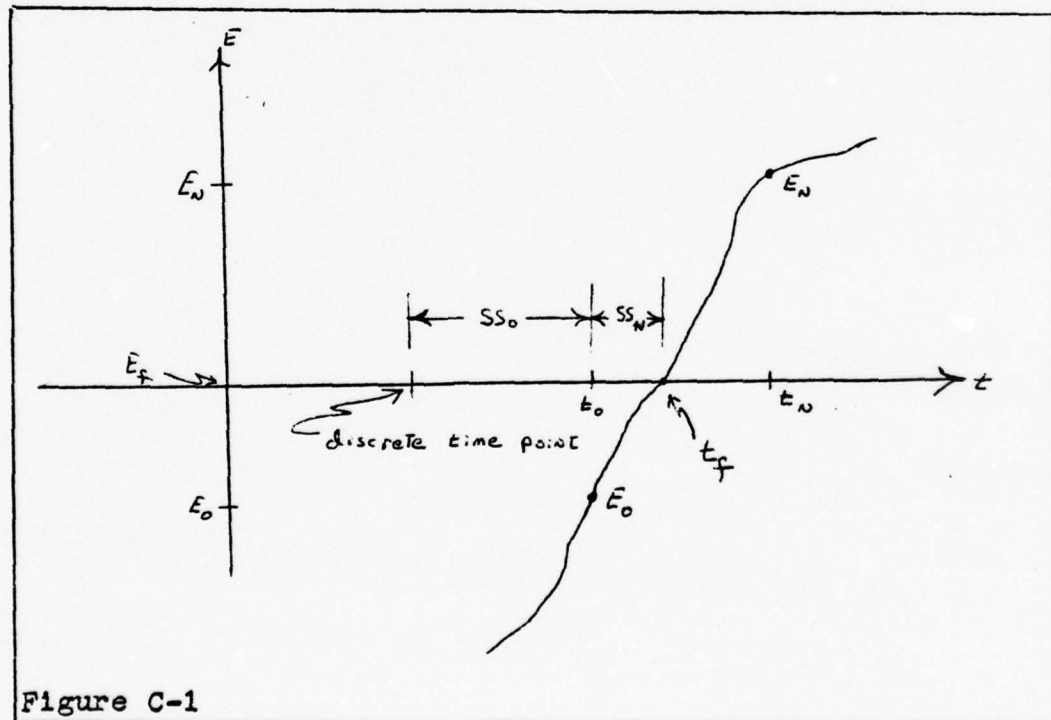


Figure C-1

APPENDIX D
Computer Program

SOLCO (Solar Control) is the name of the computer program developed to determine the optimal minimum time escape trajectory of a spacecraft propelled by solar radiation pressure. SOLCO solves the two-point boundary value problem by use of a Newton-Raphson iterator (see Appendix C). The sensitivity matrix needed in the Newton-Raphson iterator is determined by comparing neighboring trajectories to the nominal trajectory.

SOLCO is written in Fortran IV and uses double precision arithmetic. SOLCO requires a central memory core of about $60*10^3$ bytes and a CPU time of between one to six minutes on an Amdahl 470 computer. The CPU time depends mainly on the initial orbit of concern and the guess for the unknown initial co-state.

SOLCO consists of a MAIN PROGRAM and 9 subprograms. The MAIN PROGRAM and each of the subprograms are discussed separately.

MAIN PROGRAM

This is the controlling program for SOLCO.

Subprogram INPNCL

This subprogram is called by the MAIN PROGRAM. All initial data is read and constants set in this subprogram. The initial data and constants are also printed out. This initial data is read in MKS units and converted to reference orbit canonical

units where 1 DU=6378.16 km, 1 TU=806.8159 sec and $\mu = 1$ DU³/TU².

The data is read in with respect to the inertial coordinate frame as described in Chapter 3. The input variables are described below.

AC = characteristic acceleration (mm/sec²)

y(1) - y(3) = radius vector (km)

y(4) - y(6) = velocity vector (km/sec)

y(7) - y(9) = position co-state vector (sec/km)

y(10) - y(12) = velocity co-state vector (sec²/km)

prmt(1) = initial time (days), usually set equal to zero.

prmt(2) = terminating time (days) usually set large enough so that it does not interfere with the energy terminating condition.

prmt(3) = integration stepsize (days). For an orbit with a semi-major axis of 190000 km, a stepsize of 0.08 day gave good results. For a semi-major axis of 150000 km, 0.01 day was used.

EF = terminating energy condition (km²/sec²). Usually set to escape condition, EF=0.

IROT = Earth rotation factor. If the effects of the Earth's rotation about the Sun is desired, IROT should not equal zero.

IPR = Print step. The value of IPR causes every IPRth output of the Runge-Kutta subprogram to be printed; that is, IPR=1 causes every output to be printed.

INP = Plotting factor. This program has the option of storing the data from each print step on tape/file so that it can

be used later. INP equal to a non-zero number will cause storage.

KSTEP = Step size factor. KSTEP determines whether the neighboring trajectories in subprogram NEWIT are perturbed by a fractional amount of the nominal values (KSTEP=0) or by a fixed amount (KSTEP=1). KSTEP=0 was usually used.

NIMAX = Maximum number of iterations allowed in NEWIT.

FLIM = desired accuracy of the Newton-Raphson iterator. FLIM = 0.1 gave good results.

xs(1) - xs(6) = step size of the neighboring trajectories of the co-state vectors. Usually taken as 10^{-5} with KSTEP=0.

Subprogram NEWIT

This subprogram is called by the MAIN PROGRAM. This is the Newton-Raphson iterator as discussed in Appendix C. A nominal trajectory is calculated. Errors in the final co-state conditions are determined. The initial co-state vectors are varied and neighboring trajectories are calculated in order to get a six-by-six sensitivity matrix. This matrix is inverted and post-multiplied by the final co-state error in subprogram DCROUT. New values of the initial co-state vectors are obtained, and a new nominal trajectory is calculated. This is continued until the magnitude of the error in the final co-state is less than some desired accuracy (FLIM) or until convergence fails.

Subprogram DCROUT

This subprogram is called by NEWIT. Inputs to DCROUT are the six-by-six sensitivity matrix and the final co-state error vector. The sensitivity matrix is inverted and the error vector is premultiplied by this matrix. The output of this subprogram is the vector quantity by which the initial co-state should be changed.

Subprogram PRNT

This subprogram is called by NEWIT. Values of the independent and dependent variables of the iterator are printed on each iteration.

Subprogram TRAJE

This subprogram is called by NEWIT. A trajectory is calculated with the initial conditions as determined by NEWIT. This subprogram also calculates the error in the final co-state conditions.

Subprogram RK4

This subprogram is called by NEWIT and the MAIN PROGRAM. This subprogram is basically the 4th order Runge-Kutta integrator of the IBM Scientific Subroutine Package without the accuracy checks. The SSP integrator was changed slightly to allow the terminating energy condition to be satisfied.

Subprogram FIGNC

This subprogram is called by RK4. This subprogram evaluates the right hand side of the system of first order differential equations of the state and co-state. The effects of the Earth's orbit about the Sun is considered in this subprogram. The control variables (ρ and ψ) are also calculated.

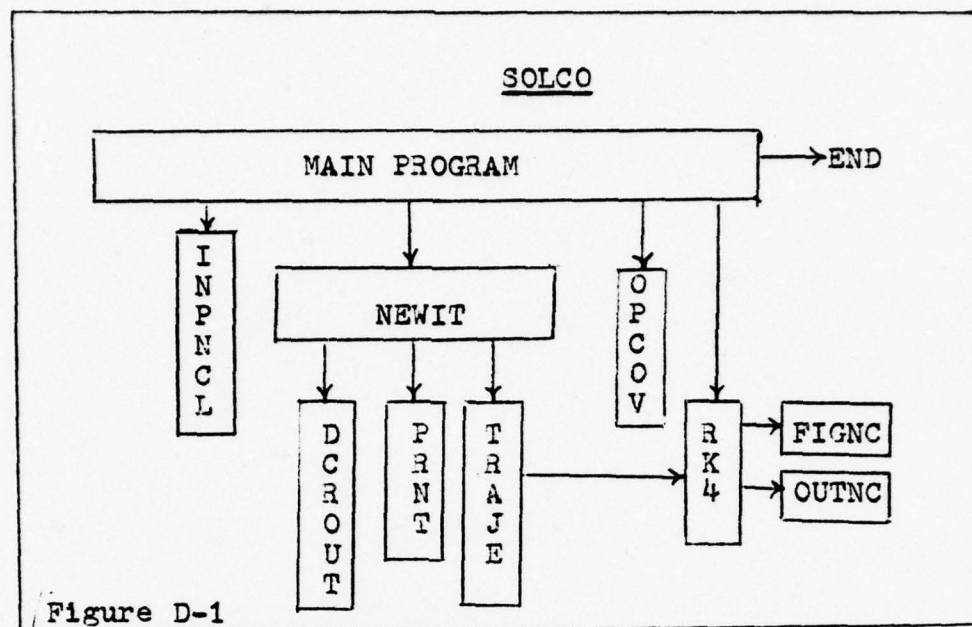
Subprogram OUTNC

This subprogram is called by RK4. The limiting energy condition is checked in this subprogram. If the terminating energy condition is exceeded, a new time step for the RK4 subprogram is determined such that the terminating energy condition is satisfied. All output is changed from reference orbit canonical units to MKS units.

Subprogram OPCOV

This subprogram is called by the MAIN PROGRAM. A summary of the converged trajectory is printed.

A flow diagram of the subprograms of SOLCO is shown below in figure D-1.



A program listing of SOLCO follows.

```

C SCLCC
C THIS IS THE CONTROLLING PROGRAM FOR FINDING THE OPTIMAL TRAJECTORY
C FOR THE PLANETARY ESCAPE PHASE OF A SPACECRAFT USING A SOLAR SAIL
C
C IMPLICIT REAL*8 (A-H,O-Z), INTEGER (I-N)
C COMMON /A/AC,C1,C2,C3,RAD,PF1,BETA,PSI,THETA,THETC,FC,DU,GM,TU,PI
C COMMON /B/ANGX1,ANGX3,EF,BETAL,FLIM,RAD3,TF,WE,GAM,ST(25)
C COMMON /IT/X(6),Z(6),XS(6),FV(6)
C COMMON /RK/PRMT(5),Y(12),DERY(12),NDIM,IHLF
C COMMON /CON/NIMAX,KSTEP,ISKIP,IC,IPR,INF
C EXTERNAL FIGNC,OUTNC,TRAJE,FRNT

C ALL SETTINGS OF CONSTANTS AND INITIAL READ AND WRITES ARE
C DONE BY THE SUBPROGRAM INPUT

C CALL INPNCL
C IF(NIMAX.EQ.0)GC TO 3
C WRITE(6,1004)

C THE PROGRAM NOW SOLVES THE 2PBP FOR THE OPTIMAL TRAJECTORY

C ISKIP=1
C CALL NEWIT(KCUNT,N1,TRAJE,PRENT)
C IF(N1.EQ.9999)WRITE(6,1003)

C A SUMMARY OF THE CONVERGED OPTIMAL TRAJECTORY IS NOW PRINTED

C WRITE(6,1005)
C CALL OPGCV(KCUNT)

C TIME HISTORY OF THE OPTIMAL TRAJECTORY IS CALCULATED AND PRINTED

C 3 ISKIP=C
C WRITE(6,1001)
C CALL RK4(PRMT,Y,DERY,NDIM,IHLF,FIGNC,CUTNC,AUX)
C IF(IHLF.GT.10)GC TC 1
C WRITE(6,1002)
C GO TO 2
C WRITE(6,1003)
C 2 STOP
C 1001 FORMAT(36H1 TIME HISTORY OF OPTIMAL TRAJECTORY)
C 1002 FORMAT(30H0 PROGRAM HAS RUN SUCCESSFULLY)
C 1003 FORMAT(29H0 OPTIMIZATION NOT SUCCESSFUL)
C 1004 FORMAT('1 THE ITERATION BEGINS')
C 1005 FORMAT('1 CONVERGED VALUES FOR THE OPTIMAL TRAJECTORY')
C END

```

```

C INPNCL
C THIS SUBPROGRAM IS CALLED BY THE MAIN PROGRAM AND READS AND
C PRINTS ALL INITIAL DATA AS WELL AS INITIAL CONSTANTS. THE INITIAL
C DATA IS READ IN THE MKS SYSTEM AND CONVERTED TO REFERENCE ORBIT
C CANONICAL UNITS. THE UNITS ARE BASED ON INTERNAL MU=1.0, INTERNAL
C DISTANCE UNIT= 1 EARTH RADII=6378.16 KM, INTERNAL TIME UNIT =
C 806.8159 SEC. AN EXTERNAL MU = 398601.2 KM*KM*SEC*SEC.

C SUBROUTINE INPNCL
IMPLICIT REAL*8 (A-H,O-Z), INTEGER (I-N)
COMMON /A/ AC,C1,C2,C3,RAD,PRI,BETA,FSI,THETA,THETC,FC,DU,GM,TU,PI
COMMON /E/ ANGX1,ANGX3,EF,BETAL,FLIM,RAD3,TF,WE,GAM,ST(25)
COMMON /IT/ X(6),Z(6),XS(6),RV(6)
COMMON /RK/ PRWT(5),Y(12),DERY(12),AUX(1,12),NDIM,IHFL
COMMON /CON/NIMAX,KSTEP,ISKIP,IC,IPR,INP

C CONSTANTS ARE SET
C
C PI=3.1415926535897932D0
DU=6.378.16D0
GM=398601.2D0
TUDSORT((DU**3.0D0)/GM)
ANGX1=90.0D0
ANGX3=90.0D0

C THE CHARACTERISTIC ACCELERATION IS ASSUMED CONSTANT (GIVEN IN MM/SEC)
READ (5,1000) AC
WRITE(6,1001) AC
WRITE(6,1003) AC

C THE CHARACTERISTIC ACCELERATION HAS TO BE CHANGED TO CANONICAL UNITS.
C AC=AC*TU*TU/(DU*1000000.0CC)
C THE STATE AND INITIAL GUESSES FOR THE CC-STATE ARE READ IN. PRINTED OUT
C AND CONVERTED TO CANONICAL UNITS. THE STATE AND CO-STATE ARE WITH
C RESPECT TO AN INERTIAL EQUATORIAL REFERENCE FRAME. THAT AT TIME=0
C HAS ITS X=AXIS POINTING AT THE SUN. THE STATE IS IN KM AND KM/SEC.
C THE CO-STATE IS IN SEC/KM AND SEC*SEC/KM.

READ(5,1013) (Y(I),I=1,3)
WRITE(6,1005)
WRITE(6,1004) (Y(I),I=1,3)
READ(5,1013) (Y(I),I=4,6)
WRITE(6,1006)
WRITE(6,1004) (Y(I),I=4,6)
READ(5,1013) (Y(I),I=7,9)

```

```

      WRITE(6,1007) (Y(I),I=7,9)
      WRITE(6,1004) (Y(I),I=10,12)
      READ(5,1013) (Y(I),I=10,12)
      WRITE(6,1008)
      WRITE(6,1004) (Y(I),I=10,12)
      DO 1 I=1,3
      1 Y(I)=Y(I)/DU
      DO 2 I=4,6
      2 Y(I)=Y(I)*TU/DU
      DO 3 I=7,9
      3 Y(I)=Y(I)*DU/TU
      DO 4 I=10,12

      4 Y(I)=Y(I)*DU/(TU*TU)

C THERE IS THE OPTION OF TERMINATING THE PROGRAM ON A TIME OR ENERGY
C CONDITION.
C
      READ(5,1027)PRMT(2),EF
      WRITE(6,1009)PRMT(2)
      PRMT(2)=PRMT(2)*86400.0D0/TU
      WRITE(6,1020)EF
      EF=EF*(TU/DU)*(TU/CU)

C THE STATE AND CO-STATE MAKE A SYSTEM OF ORDER 12
      8 NDIM=12
C NEXT THE SAIL FORCE EQUATION CONSTANTS ARE READ IN
C
      READ(5,1013) C1,C2,C3
      WRITE(6,1010) C1,C2,C3

C THE INPUT VALUES FOR THE RK4 SUBPROGRAM ARE SET
C
      READ(5,1027) PRMT(3),PRMT(1)
      WRITE(6,1011) PRMT(3)
      PRMT(3)=PRMT(3)*86400.0D0/TU
      PRMT(1)=PRMT(1)*86400.0D0/TU
      PRMT(4)=0.0D0
      PRMT(5)=0.0D0

C CALCULATE THE LIMITING VALUE OF THE CONTROL VARIABLE THETA
C
      IF(C3.EQ.0.0)GO TO 5
      C=DSQRT(C2*C2+8.0D0*C3*C3-8.0D0*C1*C3)
      A=(4.0D0*C3-C2+C)/(8.0D0*C3)
      B=-DSQRT(A)
      6 THETC=DARCOS(B)
      THET=THETC*18C.0D0/PI
      GO TO 10

```

```

5 B=DSORT((C2-C1)/(2.0D0*C2))
  GO TO 6
10 WRITE(6,1002)THEt
C
C CALCULATE THE LIMITING BETA.
C
C BETAL=THEtC-PI/2*C00
C BETAC=BETAL*180.0D0/PI
C WRITE(6,1021)BETAC
C
C THE ROTATION OF THE EARTH AROUND THE SUN IS CONSIDERED.
C
C READ(5,1014)IROT
C IF(IROT.EQ.0)GO TO 33
C W1=(66600.0D0/92900000.000)/360C.0D0
C WE=W1*TU
C WRITE(6,1025)
C WRITE(6,1026)W1,WE
C WRITE(6,1026)W1,WE
C GO TO 32
C 33 WE=0.0D0
C
C THERE IS THE OPTION OF NOT PRINTING EVERY CUTOFF OF THE RK4
C SUBPROGRAM. THE VALUE OF IPR CAUSES EVERY IPRTH OUTPUT TO BE
C PRINTED. IPR=1 WILL CAUSE EVERY OUTPUT TO BE PRINTED.
C
C 32 READ(5,1014)IPR
C WRITE(6,1015)IPR
C IC=IPR
C
C THERE IS THE OPTION OF STORING THE DATA FROM EACH PRINT STEP
C ON FILE SO THAT IT CAN BE USED LATER. IF THIS OPTION IS NOT
C DESIRED SET INP=0. INP EQUAL TO A NON-ZERO NUMBER WILL CAUSE STORAGE.
C
C READ(5,1014)INP
C IF(INP.EQ.0)GO TO 9
C WRITE(6,1019)
C
C VALUES FOR THE NEWTON-RAPHSON ITERATOR ARE SET. KSTEP DETERMINES
C IF THE STEP SIZE IS A FRACTION OF THE INITIAL VALUE (C) OR A FIXED
C VALUE (1). NIMAX IS THE MAX NUMBER OF ITERATIONS AND FLIM IS THE
C DESIRED ACCURACY. XS IS THE STEPSIZE(CANICAL UNITS IF KSTEP=1).
C
C 9 READ(5,1022)KSTEP,NIMAX,FLIM
C WRITE(6,1023)KSTEP,NIMAX,FLIM
C IF(NIMAX.EQ.0)GO TO 12
C DC 11 I=1 .6
C KK=1+6
C X(I)=Y(KK)
C Y(I)=X(I)
C 11

```

```

READ(5,1013) (XS(I),I=1,3)
READ(5,1013) (XS(I),I=4,6)
WRITE(6,1024)
WRITE(6,1004) (XS(I),I=1,3)
WRITE(6,1004) (XS(I),I=4,6)

C 1012 WRITE(6,1012)
      RETURN

C 1000 FORMAT(D25.15)
1001 FORMAT(1H1,13X,' MINIMUM TIME OPTIMAL TRAJECTORY ESCAPE ')
      R*PHASE PROGRAM FOR A SPACECRAFT POWERED BY SCALAR SAIL',//)
1002 FORMAT(27H0THE LIMITING THETA (DEG) =',1F1D25.15)
1003 FORMAT('0THE CHARACTERISTIC ACCELERATION (NM/SEC**2) =',1F1D20.6)
1004 FORMAT(1P3D25.15)
1005 FORMAT(33H0THE INITIAL RADIUS VECTOR (KM) =)
1006 FORMAT(38H0THE INITIAL VELOCITY VECTOR (KM/SEC) =)
1007 FORMAT(46H0THE INITIAL RADIUS CC-STATE VECTOR (SEC/KM) =)
1008 FORMAT(52H0THE INITIAL VELOCITY CC-STATE VECTOR (SEC*SEC/KM) =)
1009 FORMAT('0THE FINAL TIME DESIRED (DAYS) =',1F1D25.15)
1010 FORMAT(7, THE SAIL FORCE EQUATION CONSTANTS C1 =',1F1D15.5,
      R, C2 =',1P1D15.5,
      C3 =',1P1D15.5)
1011 FORMAT(52H0THE INCREMENT OF THE INDEPENDENT VARIABLE (DAYS) = ,
      R 1P1D20.8)
1012 FORMAT(7, ONE DU =6378.16C KM, ONE TL =806.8159 SEC, ,
      R, ONE MULT(GM) =398601.2 KM**3/SEC**2, )
1013 FORMAT(3D25.15)
1014 FORMAT(13)
1015 FORMAT('0THE PRINTER FACTOR =',13)
1016 FORMAT('0DATA FROM EACH PRINT STEP WILL BE STORED ON FILE')
1017 FORMAT('0THE TERMINATING ENERGY CONDITION (KM*KM/SEC*SEC) =',)
      R1D25.15
1018 FORMAT('0THE LIMITING BETA (DEG) =',1F1D25.15)
1019 FORMAT(215,2D25.15)
1020 FORMAT(215,2D25.15)
1021 FORMAT(215,2D25.15)
1022 FORMAT(215,2D25.15)
1023 FORMAT(215,2D25.15)
      NIMAX =0.15.0      FLIN =',1F1D25.15)

1024 FORMAT('0THE INCREMENTS OF THE INDEPENDENT VARIABLE FOR USE',
      R, ' IN THE ITERATOR ARE')
1025 FORMAT('0THE EARTH RATE IN (RAD/SEC) AND (RAD/TU) IS')
1026 FORMAT(1P2D25.15)
1027 FORMAT(2D25.15)
      END

```

```

C NEWIT RAPHSON ITERATOR
C SPECIAL VERSION FOR 6X6 PARTIAL DER. MATRIX. 6 DIM. Z.
C SUBROUTINE NEWIT(KOUNT,NI, FUNCT,PRTN)
C IMPLICIT REAL*8(A-F,O-Z), INTEGER (I-N)

C X-VALUES OF THE INDEPENDENT VARIABLES( INITIAL, CURRENT,FINAL).
C X-STEP SIZE TO PERTURE X TO COMPUTE PARTIAL DERIVATIVES.
C Z-VALUES OF THE DEPENDENT VARIABLES(CURRENT,FINAL)
COMMON /AAC,C1,C2,C3,RAD,PRI,RETA,PSI,THETA,THE TC,FC,DU,GM,TU,PI
COMMON /B/ANGX1,ANGX3,EF,BETAL,FLIN,FLAD3,TF,WE,GAM,ST (25)
COMMON /IT/X(6),Z(6),XS(6),RV(6)
COMMON /FK/PRNT(5),Y(12),DERY(12),AUX(1,12),NDIM,ILHF
COMMON /CN/NMAX,KSTEP,ISKIP,IC,IPR,INP
C ARRAYS USED INTERNALLY BY THE ITERATOR
C DIMENSION YNOM(6),XN(6),P(6,6),CNEF(6)
C EQUIVALENCE (YCN,CCEF)

C N= 6
NI=1
KOUNT=0
CALL FUNCT
1F(1HLF*6T*10)GO TO 95
KOUNT=KOUNT+1
FO=1*D2
DO 15 I=1,N
15 FO=FO+Z(I)**2
10 DO 16 I=1,N
XN(I)=X(I)
16 YNOM(I)=Z(I)
CALL PRTN(KOUNT,NI)
T=TF*TU/86400.0D0
WRITE(6,1017)T
WRITE(6,101)FO
1F(FO*LE,FLIM)GO TO 90
1F(NI*GT,NMAX) GO TO 30
C COMPUTE NUMERICAL PARTIAL DERIVATIVES
WRITE (6,1013)
DO 25 J=1,N
T*W=Z(J)
STFP=XS(J)*DABS(X(J))
IF ((DABS(X(J)).LT.1.0D-10).OR.(KSTEP.EQ.1))STEP=XS(J)
IF (DABS(X(J)).LT.1.D-14) WRITE (6,1014)

```

```

X(J)=X(J)+STEP
CALL FUNCT
IF(THLF.GT.10)GO TO 55
T=TF*TF 864.00 GO TO 55
WRITE(6,100)X(J),T
WRITE(6,100)X(J),T
DO 20 I=1,N
20 P(I,J)=(Z(I)-YNGM(I))/STEP
25 X(J)=TEMP
KOUNT=KOUNT+N
WRITE(6,100)N
DO 30 I=1,N
30 CONTINUE
WRITE(6,101)P(I,J),J=1,N
35 COEF(I)=-YNGM(I)
CALL DCROUT(P,CCEF,DET,0,DO,N,I,IND)
IF(IND.NE.0)GO TO 85
WRITE(6,1015)DET
DO 40 I=1,N
40 IF (CABS(COEF(I)*LT,1,DO-12).GT.EPS) COEF(I)=0,DO
WRITE(6,1003)(CCEF(I),I=1,N)
DO 50 J=1,N
50 X(J)=XN(J)+COEF(J)
51 CALL FUNCT
KOUNT=KOUNT+1
F1=0,DO
DO 52 I=1,N
52 F1=F1+Z(I)**2
WRITE(6,1010)F1
IF(F1.LT.F0)GO TO 55
WRITE(6,1008)
IF(IHALV.EQ.10) GC TO 95
IHALV=IHALV+1
DO 53 J=1,N
53 COEF(J)=(COEF(J)/2,DO)
WRITE(6,1009)COEF(J)
53 X(J)=XN(J)+COEF(J)
56 IF(NI-NIMAX).GT.70,70,80
70 NI=NI+1
F0=0
KK=0
60 TO 10
NI=9999
WRITE(6,1006)
RETURN

```

```

85 NI=9999
      WRITE(6,1007)
      RETURN
90 WRITE(6,1005)FO
      RETURN
95 NI=9999
      WRITE(6,1009)
      RETURN
1000 FORMAT(1X,1PD25.15,5X,1PD25.15)
1001 FORMAT(1X,1PD3D25.15)
1002 FORMAT(22H0 PARTIAL DERIV MATRIX)
1003 FORMAT(10 DELX ARE . ./ (1X,1PD25.15))
1005 FORMAT(5H0 F0=,1PD25.15,23H CASE CONVERGED••FERTIG)
1006 FORMAT(39H0 EXCEEDED MAXIMUM NUMBER OF ITERATIONS)
1007 FORMAT(17H0 MATRIX SINGULAR)
1008 FORMAT(1C ERROR TOO LARGE ~ NEW DELX ARE •)
1009 FORMAT(2CHC METHOD CANNOT WORK)
1010 FORMAT(5H0 F1=,1FD25.15)
1011 FORMAT(5H0 F0=,1PD25.15)
1013 FORMAT(10 X(I)+DX(I) AND FINAL TIME(DAYS) OF TRAJECTORY•
      R, FOLLOWED BY CORRESPONDING Z•)
1014 FORMAT(24H0 X(I)=0, SC DX(I)=XS(I))
1015 FORMAT(15H0 DETERMINANT =,1PD25.15)

1016 FORMAT(1/)

1017 FORMAT(•0 FINAL TIME(DAYS) OF THE TRAJECTORY =•,1PD25.15)
      END

```

```

C  DCROUT (6, DIM.)$  

SUBROUTINE DCROUT(AA,R,D,EPS,NI,M,IND)  

DOUBLE PRECISION A,R,D,EPS,I,S,P,DT,AA  

DIMENSION A(6,6),R(6,1),AA(6,6)  

5  IND=0  

N=N-1  

DO 6 I=1,N  

DO 6 J=1,N  

6  A(I,J)=AA(I,J)  

IF(M)10,25,25  

10  M=N  

DO 20 J=1,N  

DO 15 I=1,N  

15  R(I,J)=0.0D0  

20  P(I,I)=1.0D0  

25  IC=0  

11=0  

T=DABS(A(1,1))  

DO 35 I=2,N  

IF(T-DABS(A(I,1)))30,35,35  

30  II=1  

T=DAES(A(1,1))  

35  CONTINUE  

IF(II)40,65,40  

40  IC=IC+1  

IF(M)45,55,45  

45  DO 50 J=1,M  

S=P(1,J)  

R(1,J)=R(II,J)  

50  R(II,J)=S  

55  DO 60 J=1,N  

S=A(1,J)  

A(1,J)=A(II,J)  

60  A(II,J)=S  

65  P=A(1,1)  

IF(DABS(P)-EPS)70,70,75  

70  IND=1  

D=0.0D0  

60  TO 200  

75  DO 80 AC J=2,N  

80  A(1,J)=A(1,J)/P  

IF(M)85,95,85  

85  DO 90 J=1,M  

90  F(1,J)=R(1,J)/P  

95  DO 170 K=2,N  

K=N-1  

T=-1.0D0

```

```

DO 105 I=K,N
DO 68 J=1,KM
98 A(I,K)=A(I,K)-A(I,J)*A(J,K)
   TF(T-DABS(A(I,K)))100,105,105
100 T=DABS(A(I,K))
105 I=I
105 CONTINUE
105 IF(I-I-K)110,135,110
110 IC=IC+1
110 IF(M)115,125,115
115 DO 120 J=1,M
   S=R(K,J)
   P(K,J)=P(I,J)
120 P(I,J)=S
125 DO 130 J=1,N
   S=A(K,J)
   A(K,J)=A(I,J)
130 A(I,J)=S
135 DT=A(K,K)
135 IF(DABS(DT)-EPS)70,79,140
140 P=P*DT
140 IF(K-N)145,155,145
145 KP=K+1
145 DO 150 J=KP,N
148 A(K,J)=A(K,J)-A(K,I)*A(I,J)
150 A(K,J)=A(K,J)/DT
155 IF(M)160,170,160
160 DO 165 J=1,M
162 DO 162 I=1,KM
162 R(K,J)=R(K,J)-A(K,I)*R(I,J)
165 R(K,J)=R(K,J)/DT
170 CONTINUE
170 IF(MOD(IC,2))175,180,175
175 P=-P
180 P=P
180 IF(M)185,200,185
185 I=N
185 DO 190 K=2,N
190 KP=I
190 I=I-1
190 DO 190 J=1,M
190 I=KP
190 R(I,J)=R(I,J)-A(I,I)*R(I,J)
200 P=TURN
200 END

```

```

C PRNT
C THIS PROGRAM IS CALLED BY THE ITERATOR AND PRINTS THE VALUES
C OF THE INDEPENDENT AND DEPENDENT VARIABLES OF THE ITERATOR
C
C SUBROUTINE PRNT(KOUNT,NI)
C
C IMPLICIT REAL*8(A-T,O-Z)
COMMON /IT/x(6),z(6),xs(6),rv(6)
C
      WRITE (6,1001) NI,KOUNT
      WRITE (6,1002)
      WRITE (6,1003) (X(J),J=1,3)
      WRITE (6,1003) (X(J),J=4,6)
      WRITE (6,1004)
      WRITE (6,1003) (Z(J),J=1,3)
      WRITE (6,1003) (Z(J),J=4,6)
1001 FORMAT (0,0,ITERATION NUMBER =''I6'', TRAJECTORY NUMBER =''I6'')
1002 FORMAT (0,0,INDEPENDENT VARIABLES(X),)
1003 FORMAT (1X,1P3D25.15)
1004 FORMAT (0,0,DEPENDENT VARIABLES(Z),)
      RETURN
      END

```

AD-A054 754

CHARLES STARK DRAPER LAB INC CAMBRIDGE MA
OPTIMAL ESCAPE TRAJECTORY FROM A HIGH EARTH ORBIT BY USE OF SOL--ETC(U)
AUG 77 A J GREEN

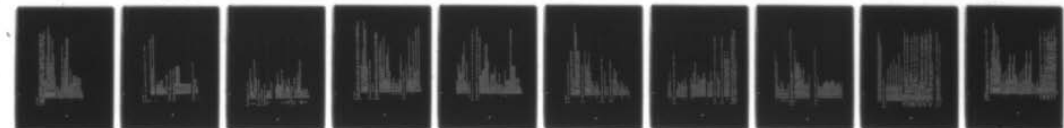
F/G 22/3

UNCLASSIFIED

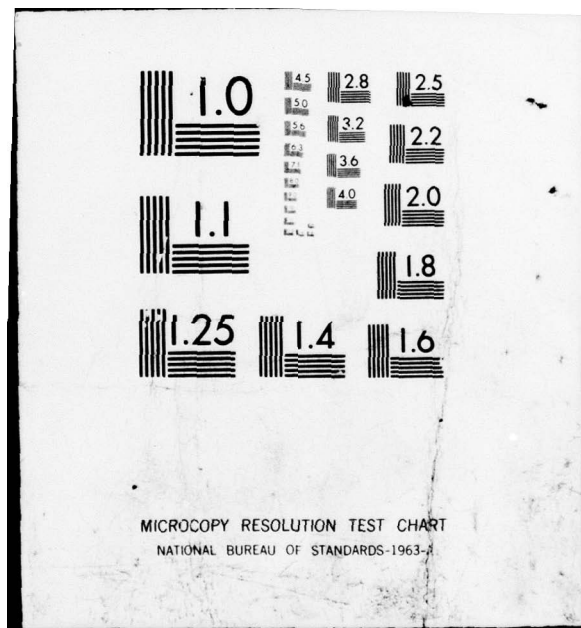
T-652

NL

2 OF 2
AD
A054754



END
DATE
FILMED
7-78
DDC



```

C TRAJE
C THIS SUBPROGRAM IS CALLED BY THE ITERATOR. A TRAJECTORY IS RUN
C WITH THE INITIAL CONDITIONS AS DETERMINED BY THE ITERATOR. THE
C TRAJECTORY IS STOPPED WHEN A TERMINAL CONDITION IS MET. THIS
C PROGRAM ALSO CALCULATES THE DEPENDANT VARIABLES OF THE ITERATOR.
C SUBROUTINE TRAJE
IMPLICIT REAL*8(A-H,C-Z),INTEGER(I-N)
COMMON /A/AC,C1,C2,C3,RAD,PRI,BETA,PSI,THETA,THETC,FC,DU,GM,TU,PI
COMMON /B/ANGX1,ANGX3,EF,BETAL,FLIM,RAD3,TF,WE,GAM,ST(25)
COMMON /IT/X(6),Z(6),XS(6),RV(6)
COMMON /RK/PRNT(5),Y(12),DERY(12),AUX(1,12),NDIM,IHLF
COMMON /CN/CON/NIMAX,KSTEP,ISKIP,IC,IPR,INF
EXTERNAL FIGNC,CUTNC
DO 1 I=1,6
Y(I)=RV(I)
K=I+6
1 Y(K)=X(I)
CALL RK4(PRNT,Y,DERY,NDIM,IHLF,FIGNC,CUTNC,AUX)
IF(IHLF.GT.10)GO TO 3
A1=(FC*DSIN(THETA))/(PRI*CSIN(BETA))
F1=(FC*DCCS(GAM)*DSIN(BETA-THETA)/DSIN(EEETA))+A1*Y(10)
F2=(FC*DSIN(GAM)*DSIN(RET-A)*DSIN(BETA-THETA)/DSIN(BETA))+A1*Y(11)
F3=A1*Y(12)
AA=Y(4)*F1+Y(5)*F2+Y(6)*F3
AB=1.0D0/RAD3
Z(1)=Y(7)-AB*Y(1)/AA
Z(2)=Y(8)-AB*Y(2)/AA
Z(3)=Y(9)-AB*Y(3)/AA
Z(4)=Y(10)-Y(4)/AA
Z(5)=Y(11)-Y(5)/AA
Z(6)=Y(12)-Y(6)/AA
3 RETURN
3 END

```

```

C RK4
C THIS IS A RUNGE KUTTA INTEGRATOR OF 4TH ORDER.
C
C SUBROUTINE RK4(FRMT,Y,DERY,NCIM,IHLF,FCT,OUTF,AUX)
C IMPLICIT REAL*8(A-H,O-Z)
C DIMENSION Y(1),DERY(1),AUX(1,1),A(4),B(4),C(4),PRMT(1)
C
C X=FRMT(1)
C XEND=PRMT(2)
C H=PRMT(3)
C PRMT(4)=0.0D0
C PRMT(5)=0.0D0
C IREC=0
C IHLF=0
C CALL FCT(X,Y,DERY)
C
C ERROR TEST
C IF (H*(XEND-X))38,37,2
C
C PREPARATION FOR R-K METHOD
C
C A(1)=.5D0
C A(2)=.252893218E1345248CC
C A(3)=.17071067811865475D0
C A(4)=.16666666666666667D0
C B(1)=2.0D0
C B(2)=1.0D0
C B(3)=1.0D0
C B(4)=2.0D0
C C(1)=.5D0
C C(2)=A(2)
C C(3)=A(3)
C C(4)=.5D0
C
C PREPARATIONS OF FIRST R-K STEP
C
C DO 3 I=1,NDIM
C   3 AUX(1+I)=0.D0
C   3 IEND=0
C

```

```

C START OF A R-K STEP
4   IS=0
    IF ((X+2*D0*H-XEND)*H)7.6.5
5   H=(XEND-X)/2.D0
6   IEND=1
7   CALL OUTP(X,Y,DERY,IHLF,NDIM,PRMT)
    IF (PRMT(5))80,8,40

C IF ENERGY IS EXCEEDED
C   80 H=PRMT(4)

C START OF R-K LOOP
8   J=1
10  AJ=A(J)
    BJ=B(J)
    CJ=C(J)
    DC 11 I=1,NDIM

R1=H*DERY(1)
R2=AJ*(R1-BJ*AUX(1,1))
Y(1)=Y(1)+R2
R2=R2+R2+R2
11  AUX(1,1)=AUX(1,1)+R2-CJ*R1
    IF (J-4)12,15,15
12  J=J+1
13  IF (J-3)13,14,13
    X=X+5D0*H
14  CALL FCT(X,Y,DERY)
    GO TO 10
C END OF R-K LOOP
C   15  CALL FCT(X,Y,DERY)
    IS=IS+1
    IF (IS.EQ.1) GO TO 7
    IF (IEND.EQ.0) GO TO 4
39  CALL OUTP(X,Y,DERY,IHLF,NDIM,PRMT)
    RETURN
40  IHLF=12
37  GC TO 39
38  IHLF=13
    GC TO 39
END

```

```

C FIGNC
C THIS SUBPROGRAM IS CALLED BY THE SUBPROGRAM RK4. THIS SUBPROGRAM
C EVALUATES THE RIGHT HAND SIDE OF THE SYSTEM OF FIRST ORDER EQUATIONS.
C

SUBROUTINE FIGNC(Q,Y,DERY)
IMPLICIT REAL*8(A-H,O-Z), INTEGER (I-N)
COMMON /AAC,C1,C2,C3,RAD,PRI,BETA,PSI,THETA,THETC,FC,DU,GM,TU,PI
COMMON /B/ANGX1,ANGX3,EF,BETAL,FLIN,FAD3,TF,WE,GAM,ST(25)
DIMENSION Y(12),DERY(12)

C CALCULATION OF THE SUN'S ROTATION
C
GAM=WE*Q

C CALCULATE THE MAGNITUDE OF THE RADIUS AND CC-STATE VECTOR
C AS WELL AS THE CLOCK AND CONE ANGLE OF THE CC-STATE VECTOR
C
RAD=DSQRT(Y(1)*Y(1)+Y(2)*Y(2)+Y(3)*Y(3))
PRI=DSQRT(Y(10)*Y(10)+Y(11)*Y(11)+Y(12)*Y(12))
IF(PRI.EQ.0.0)GO TO 1
BETA=DARCOS((DCOS(GAM)*Y(10)+DSIN(GAM)*Y(11))/PRI)
S=DSIN((BETA)
W=DCOS((GAM)*Y(11)-DSIN((GAM)*Y(10)
IF(DABS(Y(12)).LT.0.00000001DC)GC TC 2
PSI=DATAN2(W,Y(12))
GO TC 5
2 IF(W).GT.8.9
7 PSI=PI/2.0DC
GO TO 5
8 PSI=0.0DC
GO TO 5
9 PSI=PI/2.0DC
5 IF(DABS(S).LT.0.0000001DC)GO TO 1
C CALCULATE OPTIMUM THETA
C
4 IF(BETA.LT.BFTAL)GC TO 14
C=DCOS(BETA)
TT=(DSQRT(9.0DC*C*C+8.0DC*S*S)+3.0DC*C)/(4.0DC*S)
THFTN=DATAN2(TT,-1.0DC)
3 THETA=THETN
D=C1+C2*DCOS((2.0DC)*THETA)+C3*DCOS((4.0DC)*THETA)
E=DCOS((THETA-BETA)
DP=-2.0DC*C2*DSIN((2.0DC)*THETA)-4.0DC*C3*DSIN((4.0DC)*THETA)
EP=-DSIN((THETA-BFTAL)
DPP=-4.0DC*C2*DCOS((2.0DC)*THETA)-1.0DC*C3*DCOS((4.0DC)*THETA)
EPPE=-E

```

```

HF=DP*E+D*EF
HPP=DPP*E+2*CDC*DP*EP+D*EP
IF(HPP.EQ.0.CDO)GO TO 14
IF(HPP.EQ.0.CDO)GO TO 14
THETN=THETA-HP/HPP
IF(THETN.GT.PI)THETN=2*CDC*PI-THETN
IF(DABS(THETN-THETA).GE.0.000000001DC)GO TO 3
THETA=THETN
IF(THETC.GE.THETA)THETA=THETC
GO TO 12
14 THETA=THETC

C THE RIGHT HAND SIDE OF THE SYSTEM OF FIRST ORDER EQUATIONS IS
C NOW CALCULATED. THE LIMITING CONDITIONS ARE ALSO TAKEN CARE OF.

C 12 FC=AC*(C1+C2*DCOS(2.0D0*THETA)+C3*DCCS(4.0CDC*THETA))
      RAD3=RAD*RAC*RAD
      AA=DSIN(BETA-THETA)/S
      RP=DSIN(THETA)/(S*PRI)
      DERY(4)=FC*(AA*DOS(GAM)+BB*Y(10))-Y(1)/RAD3
      DERY(5)=FC*(AA*DSIN(GAM)+EE*Y(11))-Y(2)/RAD3
      DERY(6)=FC*BB*Y(12)-Y(3)/RAD3
      GC TO 1
      1 RAD3=RAD*RAD*RAD
      DERY(5)=-Y(2)/RAD3
      DERY(6)=-Y(3)/RAD3
      IF(Y(10).LT.0.CDO)GO TO 6
      THETA=THETC
      FC=0.0DC
      DERY(4)=-Y(1)/RAD3
      GO TO 11
      6 THETA=PI
      FC=AC
      DERY(4)=-FC-Y(1)/RAD3
      11 DERY(1)=Y(4)
      DERY(2)=Y(5)
      DERY(3)=Y(6)
      G=-3.0D0*(Y(10)*Y(1)+Y(11)*Y(2)+Y(12)*Y(3))/(RAD3*RAD*RAD)
      DERY(7)=G*Y(1)+Y(10)/RAD3
      DERY(8)=G*Y(2)+Y(11)/RAD3
      DERY(9)=G*Y(3)+Y(12)/RAD3
      DERY(10)=-Y(7)
      DERY(11)=-Y(8)
      DERY(12)=-Y(9)
      RETURN
      END

```

```

C OUTNC
C THIS IS THE OUTPUT PROGRAM FOR FK4
C
C SUBROUTINE OUTNC(Q,Y,DERY,ITL,F,NDIM,PRMT)
C IMPLICIT REAL*8(A-H,O-Z), INTEGER (I-N)
C PEAL*4 PLTDA(17)
COMMON /AC,C1,C2,C3,RAD,PERI,BETA,PSI,THETA,THETC,FC,DU,GM,TU,PI
COMMON /ANGX1,ANGX3,EF,BETAL,FLIM,RAD3,TF,WE,GAM,ST(25)
COMMON /C0N/NMAX,KSTEP,ISKJF,IC,IPR,INP
DIMENSION Y(12),DERY(12),PRWT(5),AID(12)

C LIMITING CONDITIONS ARE CHECKED
C
VFL=DSORT(Y(4)*Y(4)+Y(5)*Y(5)+Y(6)*Y(6))
FN=VEL*VEL/2.000-1.0D0/RAD
IF (PRMT(4)*NE*0.0D0) GO TO 20
IF (DARS(EN)*LT*0.0000000001D0) GO TO 20
IF (EN.GT.EFF) GO TO 21
DO 12 I=1,12
ST(I)=Y(I)
K=I+12
12 ST(K)=DERY(I)
ST(25)=EN
TF=Q

C DETERMINATION IF THIS IS A PRINT STEP
C
6 IF (IC*GE*IPR) GO TO 10
  IC=IC+1
  GO TO 11

C IF THE ENERGY CONDITION IS EXCEEDED
C
21 PRWT(5)=-3.0D0
  SL0PF=(EN-ST(25))/(C-TF)
  PRMT(4)=-ST(25)/SLOPE
  DO 14 I=1,12
    Y(I)=ST(I)
  14 K=I+12
    DERY(I)=ST(K)
    FN=ST(25)
    Q=TF
    GAM=WE*0
    GO TO 11
20  TF=Q

```

```

      PRINT(5)=3.0DC
      10 IF(1ISKIP.EQ.1)GC TO 11
      IC=1

C CONVERT FROM INTERNAL UNITS TO OUTPUT UNITS
C

      TS=Q*TU
      TH=TS/3600.0D0
      TD=TH/24.0D0
      DO 1 I=1,3
      1 AID(I)=Y(I)*DU
      DO 2 I=4,6
      2 AIC(I)=Y(I)*DU/TU
      DO 3 I=7,6
      3

      3 AID(I)=Y(I)*TU/DU
      DO 4 I=10,12
      4 AID(I)=Y(I)*(TU*TU)/DU
      FCC=FCC*(DU*1.0D0*0.0D0)/(TU*TU)
      RADC=RAD*DU
      PRIC=PRI*(TU*TU)/DU
      VELC=VEL*DU/TU
      R=RETA*180.0DC/P1
      P=PSI*180.0DC/P1
      THETD=THETA*180.0DQ/P1
      GC=GAM*180.0D0/P1

      C
      WRITE(6,100C)
      WRITE(6,1001)
      WRITE(6,1002)Q,T,S,TH,TD
      WRITE(6,101)GC

C THE ENERGY OF THE SPACECRAFT IS CONVERTED TO OUTPUT UNITS
C
      FNC=FN*(DU/TU)*(DL/TU)
      WRITE(6,1014)ENC

C CALCULATION OF THE SPHERICAL COORDINATES OF THE SPACECRAFT
C
      1 IF(DABS(Y(1)).LT.C.CC0CC0CC0D0)GO TO 32
      ANGX1=DATAN2(Y(2)*Y(1)*180.0D0/P1
      32 IF(DARS(Y(3))*L1*0.0D0*0.0D0*0.0D0)GO TO 33
      ANGX3=DATAN2(Y(2)*Y(3))*180.0D0/P1

C CALCULATION OF THE CLOCK ANGLE OF THE CHARACTERISTIC FORCE
C WITH RESPECT TO THE VELOCITY VECTOR COMPONENT IN THE X2-X3 PLANE
C PLANE (PSIV). THE CLOCK ANGLE WITH RESPECT TO THE X3 AXIS (PSI)
C WAS CALCULATED IN THE SUBPROGRAM FIG.

```

```

C 33 IF(DARS(Y(6)).LT.0.000000000000000)GO TO 34
C ANG=DATAN2(Y(5).Y(6))*180.0D0/PI
C PSIV=P-ANGV
C GO TO 35
C 34 IF(Y(5))36,37,38
C 36 PSIV=P-270.0D0
C GO TO 35
C 37 PSIV=P
C GO TO 35
C 38 PSIV=P-90.0D0

C THE ANGULAR MOMENTUM, SEMI-MAJOR AXIS, ECCENTRICITY AND PERICENTER
C OF THE ORBIT ARE DETERMINED
C
C 35 IF(DARS(FNC).LT.0.000000000000000)GO TO 50
C
C Z1=(AID(2)*AID(6)-AID(3)*AID(5))
C Z2=(AID(1)*AID(6)-AID(3)*AID(4))
C Z3=(AID(1)*AID(5)-AID(2)*AID(4))
C H=DSQRT(Z1*Z1+Z2*Z2+Z3*Z3)
C AE=GM/(2.0D0*ENC)
C AEH=DARS(1.0D0)-(H**H)/(GM**A)
C F=DSQRT(AEH)
C R=A*(1.0D0-E)
C WRITE(6,1017)
C WRITE(6,104)H,A,E,F
C

C THE DATA IS STORED TO BE USED LATER FOR PLOTTING
C
C 50 IF(INP.EQ.0)GO TO 40
C
C PLTDA(1)=TS
C PLTDA(2)=A
C PLTDA(3)=E
C PLTDA(4)=RADC
C PLTDA(5)=AID(1)
C PLTDA(6)=AID(2)
C PLTDA(7)=AID(3)
C PLTDA(8)=VELC
C PLTDA(9)=AID(4)
C PLTDA(10)=AID(5)
C PLTDA(11)=AID(6)
C PLTDA(12)=PRIC
C PLTDA(13)=H
C PLTDA(14)=FCC
C PLTDA(15)=THFTD
C PLTDA(16)=P
C PLTDA(17)=PSIV

```

1017 FORMAT("THE H(KM*KM/SEC). A(KM). E AND PERICENTER RADIUS(KM).",
1018 P, "OF THE ORBIT ARE.")
1019 FORMAT("THE DIRECTION OF THE SUN (DEG) =", P)
END

C OPCOV PROGRAM IS CALLED BY THE MAIN PROGRAM AND PRINTS A SUMMARY
 C THIS PROGRAM IS CALLED BY THE MAIN PROGRAM AND PRINTS A SUMMARY
 C OF THE CONVERGED TRAJECTORY DATA

```

SUBROUTINE OPCOV (KCOUNT)
  IMPLICIT REAL*8 (A-H,O-Z), INTEGER (I-N)
  COMMON /A/AC,C1,C2,C3,RAD,PRI,BETA,PSI,THETA,THETC,FC,DU,GM,TU,PI
  COMMON /B/ANGX1,ANGX3,EF,BETAL,FLIM,FLAC3,TF,WE,GAM,ST(25)
  COMMON /IT/X(6),Z(6),XS(6),RV(6)
  COMMON /RK/PRNT(5),Y(12),DERY(12),AUX(1*12),NDIM,IHLF
  COMMON /CON/NIMAX,KSTEP,ISKIP,IC,IPR,INF
  DIMENSION AMBA(6),ERRCR(6)
  DO 1 I=1*3
  1 AMBA(1)=X(1)*TU/DU
  DO 2 I=4*6
  2 AMBA(1)=X(1)*TU*TU/DU
  WRITE(6,1000)
  WRITE(6,1001)X(1)*X(2)*X(3)
  WRITE(6,1001)AMBA(1),AMBA(2),AMBA(3)
  WRITE(6,1002)
  WRITE(6,1001)X(4)*X(5)*X(6)
  WRITE(6,1001)AMBA(4),AMBA(5),AMBA(6)
  TF=TF*TU/86400.0D0
  WRITE(6,1003)TF
  DO 7 I=1*3
  7 ERROR(1)=Z(1)*TU/DU
  DO 8 I=4*6
  8 ERROR(1)=Z(1)*TU*TU/DU
  WRITE(6,1004)
  WRITE(6,1001)Z(1)*Z(2)*Z(3)
  WRITE(6,1001)ERROR(1),ERROR(2),ERROR(3)
  WRITE(6,1005)
  WRITE(6,1001)Z(4)*Z(5)*Z(6)
  WRITE(6,1001)ERRCR(4),ERRCR(5),ERROR(6)
  DO 9 I=1*6
  Y(1)=RV(1)
  K=I+6
  9 WRITE(6,1007)
  RETURN
  1000 FORMAT('0THE OPTIMAL INITIAL RADIIUS CO-STATE VECTOR IN ',  

    R, 'CANONICAL AND MKS UNITS.')
  1001 FORMAT(1P3D25.15)
  1002 FORMAT('0THE OPTIMAL INITIAL VELOCITY CO-STATE VECTOR IN ',  

    R, 'CANONICAL AND MKS UNITS.')
  1003 FORMAT('0THE FINAL MINIMUM TIME(DAYS) = ',1F10.25*15)
  1004 FORMAT('0THE ERROR (ACTUAL-DESIRED) IN THE FINAL RADIUS.',  

    R, 'CO-STATE VECTOR IN CANONICAL AND MKS UNITS.')
  1005 FORMAT('0THE ERROR (ACTUAL-DESIRED) IN THE FINAL VELOCITY.',  

    R, 'CO-STATE VECTOR IN CANONICAL AND MKS UNITS.')
  1007 FORMAT('0THE FINAL CONVERGED VALUES OF THE STATE AND COSTATE.',  

    R, 'ARE LISTED IN THE FOLLOWING OPTIMAL TIME HISTORY.')
  END

```